Revised MS submitted to HESS

Deleted: *Confidential*

Evaluation of Lacustrine Groundwater Discharge, Hydrologic Partitioning, and Nutrient Budgets in a Proglacial Lake in Qinghai-Tibet Plateau: Using ^{222}Rn and Stable Isotopes

Xin LUO[1, 2], Xingxing Kuang[3], Jiu Jimmy Jiao[1, 2*], Sihai Liang[4], Rong Mao[1, 3], Xiaolang Zhang[1, 3], and Hailong Li[3]

Deleted: X

[1]Department of Earth Sciences, The University of Hong Kong, P. R. China

[2]The University of Hong Kong, Shenzhen Research Institute (SRI), Shenzhen, P. R. China

[3] School of Environmental Science and Engineering, Southern University of Science and Technology, 1088 Xueyuan Rd., Shenzhen, China

Deleted: School of Environmental Scie and Engineering, South University of Science and Technology of China (SUS Shenzhen, China.

[4]School of Water Resources & Environment, China University of Geosciences, 29 Xueyuan Road, Beijing, China

Corresponding author: Jiu Jimmy Jiao (jjiao@hku.hk)

Department of Earth Sciences, The University of Hong Kong

Room 302, James Lee Science Building, Pokfulam Road, Hong Kong

Tel (852) 2857 8246; Fax (852) 2517 6912

Abstract

Proglacial lakes are good natural laboratories to investigate groundwater and glacier dynamics under current climate condition and to explore biogeochemical cycling under pristine lake status. This study conducted a series of investigations of ^{222}Rn, stable isotopes, nutrients and other hydrogeochemical parameters in Ximen Co Lake, a remote proglacial lake in the east of Qinghai-Tibet Plateau (QTP). A radon mass balance model was used to quantify the lacustrine groundwater discharge (LGD) of the lake, leading to an LGD estimate of 10.3 ± 8.2 mm d^{-1}. Based on the three end member models of stable ^{18}O and Cl^-, the hydrologic partitioning of the lake is obtained, which shows that groundwater discharge only accounts for 7.0 % of the total water input. The groundwater derived DIN and DIP loadings constitute 42.9 % and 5.5 % of the total nutrient loading to the lakes, indicating the significance of LGD in delivering disproportionate DIN into the lake. This study presents the first attempts to evaluate the LGD and hydrologic partitioning in the glacial lake by coupling radioactive and stable isotopic approaches and the findings advance the understanding of nutrient budgets in the proglacial lakes of QTP. The study is also instructional in revealing the hydrogeochemical processes in proglacial lakes elsewhere.

Keywords: Proglacial lake; ^{222}Rn; lacustrine groundwater discharge; hydrologic partitioning; nutrient budgets

Deleted: primary productivity

Deleted: The primary productivity of th lake water is calculated to be 0.41 mmol m^{-2} d^{-1}.

Deleted: and primary productivity

Deleted: ; primary productivity

1. Introduction

High altitude and latitude areas are intensively influenced by the melting of glaciers due to climatic warming. Of particular importance are the proglacial areas, such as proglacial lakes and moraines, because they are particularly affected by climatic change induced glacier retreating and thawing of permafrost (Barry 2006, Heckmann et al. 2015, Slaymaker 2011). The proglacial lakes are usually located close to ice front of a glacier, ice cap or ice sheet, with the vicinity to the ice front sometimes defined as the areas with subrecent moraines and formed by the last significant glacier advances at the end of the Little Ice Age (Barry 2006, Harris et al. 2009, Heckmann et al. 2015, Slaymaker 2011). These lakes are located in the transition zones from glacial to non-glacial conditions, and can serve as natural laboratories to explore hydrological processes, biogeochemical cycles and geomorphic dynamics under current climatic conditions (Dimova et al. 2015, Heckmann et al. 2015).

The Qinghai-Tibet Plateau (QTP), the third pole of the world, serves as the water tower of most of the major rivers in Asian (Qiu 2008). Unique landscapes such as endorheric lakes, permafrost, glaciers, and headwater fluvial networks are developed due to the intensive interaction between the atmosphere, hydrosphere, biosphere and cryosphere (Lei et al. 2017,

Deleted: Proglacial

Deleted: providing

Deleted: (Qiu 2008)

Deleted: coherent

Yao et al. 2013, Yao et al. 2012, Zhang et al. 2017a, Zhang et al. 2017b). Distributed mountainous glaciers and lakes are the most representative landscapes and are highly sensitive to the climate changes. In the past decade, the lakes in the interior of the QTP show overall expanding with respect to an overall increase of precipitation, accelerated glacier melting and permafrost degradation (Heckmann et al. 2016, Yang et al. 2014, Zhang et al. 2017a, Zhang et al. 2017b, Zhang et al. 2013). Some latest studies have made effects to depict the hydrologic partitioning of the majority of the lakes in the QTP based on long term observation of climatological parameters, and remote sensing approaches. However, so far a quantitative evaluation of the water balance and hydrologic partitioning, especially the groundwater component of the lakes in the QTP is limited due to the scarcity of observational data. Therefore, there is a great need to conduct refined and systematical field observation to provide groundtruth dataset and tenable models to depict the water balance and hydrologic partitioning of the lakes, especially proglacial lakes in the QTP (Yang et al. 2014, Zhang et al. 2017b).

Mountainous proglacial lakes, formed by glacial erosion and filled by melting glaciers, are widely distributed in the Qinghai-Tibet Plateau (QTP), especially along the substantial glacier retreating areas of Himalaya Mountains (MT.), Qilian MT., Tienshan MT., etc. Characterized by higher elevations, small surface areas but relatively large depths, mountainous proglacial lakes in QTP lack systematic

Deleted: and deepening

Deleted: as far as now,

Deleted: refining and

Deleted: led

Deleted: ed

Deleted:

field-based hydrological studies due to their remote locations and difficulty in conducting field work (Bolch et al. 2012, Farinotti et al. 2015, Yao et al. 2012).

There has been extensive recognition of the importance of groundwater discharge to various aquatic systems for decades (Dimova and Burnett 2011, Johannes 1980, Valiela et al. 1978). Very recently, the topic of 'lacustrine groundwater discharge (LGD)', which is comprehensively defined as groundwater exfiltration from lake shore aquifers to lakes (Blume et al. 2013, Lewandowski et al. 2015, Lewandowski et al. 2013, Rosenberry et al. 2015), has been introduced. LGD is analogous of in submarine groundwater discharge (SGD) in coastal environments. LGD plays a vital role in lake hydrologic partitioning, which is defined as the separation of groundwater discharge/exfiltration, riverine inflow, riverine outflow infiltration, surface evaporation and precipitation for the hydrological cycle of the lake (Good et al. 2015, Luo et al. 2017). LGD also serves as an importance component in delivering solutes to lakes since groundwater is usually concentrated in nutrients, CH_4, dissolved inorganic/organic carbon (DIC/DOC) and other geochemical components (Belanger et al. 1985, Dimova et al. 2015, Lecher et al. 2015, Paytan et al. 2015). Nutrients and carbon loading from groundwater greatly influences ratios of dissolved inorganic nitrogen (DIN) to dissolved inorganic phosphate (DIP) (referred as N: P ratios thereafter), ecosystem structure and the primary productivity of the lake aquatic

Formatted: Font: 11 pt

system (Belanger et al. 1985, Hagerthey and Kerfoot 1998, Nakayama and Watanabe 2008).

LGD studies utilize various methods including direct seepage meters (Lee 1977, Shaw and Prepas 1990), geo-tracers such as radionuclides, stable ^{2}H and ^{18}O isotopes (Gat 1995, Kluge et al. 2007, Kraemer 2005, Lazar et al. 2008), heat and temperature (Liu et al. 2015, Sebok et al. 2013), numerical modeling (Smerdon et al. 2007, Winter 1999, Zlotnik et al. 2009, Zlotnik et al. 2010) and remote sensing (Anderson et al. 2013, Lewandowski et al. 2013, Wilson and Rocha 2016). Recently, some researchers started to investigate groundwater dynamics in peri- and proglacial areas, mostly based on the approaches of numerical modeling (Andermann et al. 2012, Lemieux et al. 2008a, Lemieux et al. 2008b, Lemieux et al. 2008c, Scheidegger and Bense 2014). However, the quantification of groundwater and surface water exchange in proglacial lakes is still challenging due to limited hydrogeological data and extremely seasonal variability of aquifer permeability (Callegary et al. 2013, Dimova et al. 2015, Xin et al. 2013).

^{222}Rn, a naturally occurring inert gas nuclide highly concentrated in groundwater, can be more applicable in fresh aquatic systems and has been widely used as a tracer to quantify groundwater discharge in fresh water lakes (Corbett et al. 1997, Dimova et al. 2015, Dimova and Burnett 2011, Dimova et al. 2013, Kluge et al. 2007, Kluge et al.

2012, Luo et al. 2016, Schmidt et al. 2010) and terrestrial rivers and streams (Batlle-Aguilar et al. 2014, Burnett et al. 2010, Cook et al. 2006, Cook et al. 2003). Of particular interest are investigations of temporal ^{222}Rn distribution in lakes, since it can be used to quantify groundwater discharge and reflect the locally climatological dynamics (Dimova and Burnett 2011, Luo et al. 2016). Temporal radon variations give high resolution estimates of groundwater discharge to lakes over diel cycles, allowing evaluation of LGD and the associated chemical loadings. However, there has been no study of radon-based groundwater discharge in mountainous proglacial lakes, especially for those lakes in the QTP.

This study aims to investigate the groundwater surface water interactions for the proglacial lake of Ximen Co, by estimating the LGD and evaluating the hydrologic partitioning of the lake. LGD is estimated with ^{222}Rn mass balance model, and the hydrologic partitioning of the lake is obtained with the three endmember model coupling the mass balance of water, stable isotopes and Cl^-. Moreover, LGD derived nutrients are estimated and the nutrient budgets of the lake are depicted. This study, to our knowledge, makes the first attempt to quantify the LGD, hydrologic partition, and groundwater borne nutrients of the proglacial lake in QTP and elsewhere via the approach integrating multiple tracers. This study provides insights of hydrologic partitioning in a typical mountainous proglacial lake under current climate condition

Deleted: Then,

Deleted: Finally, primary productivity o
the lake water is calculated based on the
nutrient budgets.

and reveals groundwater borne chemical loadings in this proglacial lake in QTP and elsewhere.

2. Methodology

2.1 Site descriptions

The Nianbaoyeze MT., located at the eastern margin of the QTP and being the easternmost part of NW-SW trending Bayan Har Shan, is situated at the main water divide of the upper reaches of Yellow River and Yangtze River (Figure 1). With a peak elevation of 5369 m, the mountain rises about 500-800 m above the surrounding peneplain and displays typical Pleistocene glacial landscapes such as moraines, U-shaped valleys and cirques (Lehmkuhl 1998, Schlutz and Lehmkuhl 2009, Wischnewski et al. 2014). The present snow line is estimated to be at an elevation of 5100 m (some updated references) (Schlutz and Lehmkuhl 2009). Controlled by the South Asia and East Asia monsoons, the mountain has an annual precipitation of 975 mm in the southern part and 582 mm in the northwestern part, with 80 % occurring during May and October (Yuan et al. 2014, Zhang and Mischke 2009). The average temperature gradient is about 0.55 ^{o}C per 100 m, and the closest weather station, locating in Jiuzhi town (N: 33.424614°, E: 101.485998) at the lower plains of the mountain, recorded a mean annual temperature of 0.1 ^{o}C. Snowfalls occur in nearly

10 months of the entire year and there is no free-frost all year around (Böhner 1996, 2006, Schlutz and Lehmkuhl 2009). The precipitation, daily bin-averaged wind speed and temperature in Aug, 2015 were recorded to be 90 mm, 0.7 m s^{-1} and 9.5 ^oC from Jiuzhi weather station (Figure 2). The water surface evaporation was recorded to be 1429.8 mm in 2015 from Jiuzhi weather station.

Among the numerous proglacial lakes developed in the U-shaped valleys of the Nianbaoyeze MT., Ximen Co lake is located at the northern margin of the mountain with an elevation of 4030 m asl, and is well studied and easily accessible (Lehmkuhl 1998, Schlutz and Lehmkuhl 2009, Yuan et al. 2014, Zhang and Mischke 2009). The lake was formed in a deep, glacially eroded basin with a catchment area of 50 km^2, and has a mean and a maximum depth of 40 m and 63.2 m, and a surface area of 3.6 km^2. The vegetation around the lake is dominated by pine meadows with dwarf shrubs, rosette plants and alpine cushion (Schlutz and Lehmkuhl 2009, Yuan et al. 2014, Zhang and Mischke 2009). Mostly recharged by the glacial and snowpack melting water and regional precipitation, the lake is stratified with an epilimnion depth about 4.4 m in the summer time. The lake is usually covered by ice in the winter time (Zhang and Mischke 2009). The superficial layer within the U-shaped valley is characterized by peat, clay and fluvial gravels with a depth about 1-3.5 m. Discontinuous and isolated permafrost is present at the slope of the valley above the elevation of about 4150 m. The maximum frozen depth is about 1.5 m for the seasonal frozen ground around the lake. The seasonal frozen ground serves as an unconfined aquifer during the unfrozen months from July to October, and groundwater discharges into the epilimnion of the lake (Schlutz and Lehmkuhl 2009, Wang 1997, Zhang and Mischke 2009).

2.2 Sampling and field analysis

The field campaign to Ximen Co Lake was conducted from August, 2015, when it is warm enough to take the water samples of different origins as the studied site is seasonally frozen. A ^{222}Rn continuous monitoring station was setup at the southeast part of the lake, which is fairly flat for setting up our tent and monitoring system. Surface water samples were collected around the lake, rivers at the upstream and downstream. Porewater samples were collected at one side of the lake as the other side is steep and rocky. The basic water quality parameters of conductivity (EC), dissolved oxygen (DO), TDS, ORP, pH in the water were recorded with the multi-parameter meter (HANNA, Co.). Relative humidity was recorded with a portable thermo-hydrometer (KTH-2, Co.). Lake water samples were taken with a peristaltic pump into 2.5 L glass bottles for ^{222}Rn measurement with the Big Bottle system (Durridge, Co.). Surface water samples were filtered with 0.45 μm filters

(Advantec, Co.) in situ and taken into 5 ml, 15 ml, 15 ml and 50 ml Nalgene centrifugation tubes for stable isotope, major anion, cation and nutrient analysis. Porewater samples were taken from the lakes shore aquifers with a push point sampler (M.H.E, Co.) connected to peristaltic pump (Solinst, Co.) (Luo et al. 2014, Luo et al. 2016). 100 ml raw surface water or porewater was titrated with 0.1 μM H_2SO_4 cartridge (Hach, Co.) in situ to measure total alkalinity (Hasler et al. 2016, Warner et al. 2013, White et al. 2016). Porewater was filtered with 0.45 μm syringe filters (Advantec, Co.) in situ and taken into 5 ml, 15 ml, 15 ml and 50 ml Nalgene centrifugation tubes for stable isotope, major anion, cation and nutrient analysis. 250 ml porewater was taken for ^{222}Rn measurement with RAD7 H_2O (Durridge, Co.) Samples for major cation analysis were acidified with distilled HNO_3 immediately after the sampling.

^{222}Rn continuous monitoring station was set up at the northwest of the lake, close to the downstream of the lake (Figure 1b). Lake water (about 0.5 m) was pumped with a DC pump (12 V) driven by lithium batteries (100 Ah) and sprinkled into the chamber of RAD7 AQUA with a flow rate > 2 L min^{-1}, where ^{222}Rn in water vapor was equilibrated with the air ^{222}Rn. The vapor in the chamber was delivered into two large dry units (Drierite, Co) to remove the moisture and circulated into RAD7 monitor, where ^{222}Rn activities were recorded every 5 mins. A temperature probe

Deleted: L

(HOBO$^{@}$) was insert into the chamber to record the temperature of the water vapor. The monitoring was performed from 11: 31 am, Aug 22^{nd} to 6: 30 am, Aug 24^{th}, 2015. During the period of 1:50-4:30 pm on Aug 22^{nd}, a sudden blizzard occurred, leading to an hourly precipitation about 0.6 mm to the lake area. Daily and hourly climatological data such as wind speed, air temperature and precipitation were retrieved from the nearest weather station in Jiuzhi town (N: 33.424614°, E: 101.485998). Moreover, another RAD7 was placed at the lakeshore to measure ^{222}Rn in the ambient air around the lake. Due to extremely low activities, the monitoring period was conducted only for 4 hours, and the mean activity was adopted as the background radon-222 activity to be used in the mass balance model. Water level and temperature fluctuations were recorded with a conductivity-temperature-depth diver (Schlumberger, Co.) fixed at about 20 cm below the lake surface and calibrated with local atmospheric pressure recorded by a baro-diver (Schlumberger, Co.) above the lake. To correct for dissolved ^{226}Ra supported ^{222}Rn, one radium sample was extracted from 100 L lake water with MnO_2 fiber as described elsewhere (Luo et al. 2014, Moore 1976).

2.3 Chemical analysis

Major ions were measured with ICS-1100 (Dionex. Co.) in the Department of Earth

Deleted: monitor

Deleted: set

Formatted: Superscript

Deleted: s

Deleted: er

Deleted: when constructing

Sciences, the University of Hong Kong. The uncertainties of the measurements are less than 5 %. Nutrients, DIN and DIP were analyzed with flow injection analysis equipped with auto-sampler (Lachat. Co.) in the School of Biological Sciences, the University of Hong Kong. Stable ^{18}O and ^{2}H isotopes were measured with MOA-ICOS laser absorption spectrometer (Los Gatos Research (LGR) Triple Isotope Water Analyzer (TIWA-45EP)) at State Key Laboratory of Marine Geology, Tongji University, Shanghai. The stable isotopic standards and the recovery test has been fully described elsewhere (Luo et al., 2017). The measurement uncertainty is better than 0.1 % for ^{18}O and 0.5 % for ^{2}H. ^{226}Ra was detected with RAD7 with the method described elsewhere (Kim et al. 2001, Lee et al. 2012, Luo et al. 2018).

2.4 Radon transient model

Previous studies employed a steady state radon-222 mass balance model to quantify LGD to lentic system such as lakes and wetlands (Dimova and Burnett 2011, Luo et al. 2016). This model assumes that radon input derived from groundwater inflow, diffusion and river inflow are balanced by the radon losses of atmospheric evasion, decay and river outflow. However, recent studies revealed that the steady state is mainly reached after 2-15 days of constant metrological conditions, and mostly lentic system can be not be treated as steady state due to rapid radon-222

Deleted: ly

degassing to the atmosphere driven by wind-induced turbulence (Gilfedder et al., 2015; Dimova and Burnett, 2011).

Ximen Co lake is demonstrated to be highly stratified with an epilimnion of 4.4 m (Zhang and Mischke 2009). The lake was formed by glacier erosion and the lakebed is characterized by granite bedrock with a thin sedimentary clay layer. Previous studies have indicated that sediment with a thickness of 0.7-3.3 m has been developed on the bedrock and forms the lake shore aquifer, which consists of clay, soils and gravels (Schlutz and Lehmkuhl 2009). Porewater sampled in the aquifer immediately behind the lake shore can well represent groundwater discharging into the lake, as suggested previously (Lewandowski et al. 2015, Rosenberry et al. 2015, Schafran and Driscoll 1993). LGD has been widely considered to occur within the first few meters of the lake shore (Lee et al. 1980, Rosenberry et al. 2015, Schafran and Driscoll 1993) and groundwater is considered to predominately discharge into the epilimnion since deep groundwater flow is highly limited by the Precambrian bedrock (Einarsdottir et al., 2016). Therefore, ^{222}Rn mass balance model is established to quantify LGD to the epilimnion from the lake shore. Due to negligible hydrological connection between the epilimnion and hypolimnion, LGD for the lake can be quantified with ^{222}Rn mass balance model for the epilimnion.

The governing equation of radon-222 transient mass balance model within a 1 x

1 x z cm (where z is the depth in cm) can be expressed as (Gilfedder et al. 2015):

$$z\frac{\partial I_{\mathrm{w}}}{\partial \mathrm{t}} = F_{gw} + (I_{^{226}Ra} - I_{\mathrm{w}}) \times z \times \lambda_{222} + F_{diff} - F_{atm} \qquad (1)$$

where F_{gw}, F_{diff}, F_{atm} [Bq m^{-2} d^{-1}] are ^{222}Rn loadings from LGD, water-sediment diffusion and water-air evasion, respectively; z [m] is the lake water level depth recorded by the diver. λ_{222} is the decay constant of ^{222}Rn with a value of 0.186 d^{-1}. $\lambda_{222} \times I_{^{226}Ra}$ and $\lambda_{222} \times I_{w}$ account for the production and decay of ^{222}Rn [Bq m^{-2} d^{-1}] in the water column, respectively. I_{w} and $I_{^{226}Ra}$ [Bq m^{-2}] represent ^{222}Rn and ^{226}Ra inventories in the epilimnion, and are expressed as: $I_{\mathrm{w}} = H \times C_{\mathrm{w}}$ and $I_{^{226}Ra} = H \times C_{^{226}Ra}$, respectively; where H [m] is the depth of the epilimnion; C_{w} and $C_{^{226}Ra}$ is the ^{222}Rn and ^{226}Ra activity [Bq m^{-3}], respectively.

The model is valid under the following assumptions: 1) The epilimnion is well mixed which is the actual condition for most natural boreal and high altitude glacial lakes (Åberg et al. 2010, Zhang and Mischke 2009). 2) ^{222}Rn input from riverine water inflow, and loss from the lake water outflow and infiltration into the lake shore aquifer is negligible compared to the groundwater borne ^{222}Rn, because ^{222}Rn concentration of groundwater is 2-3 orders of magnitude larger than that lake water (Dimova and Burnett 2011, Dimova et al. 2013). Generally, ^{222}Rn in the epilimnion is sourced from LGD and decay input from parent isotope of ^{226}Ra under secular equilibrium, and is mainly lost via atmospheric evasion and radioactive decay.

F_{atm} is the key sinking component of the transient model and is finally a function of wind speed and water temperature, both of which are temporal variant variables (Supplementary information). Lake water level z is also a temporal variant variable which represents the fluctuations of water volume of the epilimnion. This equation is discretized by the forward finite difference method, and the groundwater flux at each time step can be solved as follow

$$[{}^{222}Rn_{t+\Delta t}] = \frac{[z \times {}^{222}Rn_t + [F_{diff} + F_{gw} - F_{atm} - {}^{222}Rn_t \times \lambda \times z] \times \Delta t}{z} \quad (2)$$

where ${}^{222}Rn_{t+\Delta t}$ and ${}^{222}Rn_{t+\Delta t}$ [Bq m^{-3}] is the ^{222}Rn activity at current time step and at the previous time steps, respectively, and Δt [min] is the time step which is set to be 5 min in consistence with the ^{222}Rn record interval. With the inverse calculation based on Equation (2), the groundwater inflow at each time step can be obtained. However, large errors of the final LGD calculation will be induced by even a small amount of noise in the measured ^{222}Rn data due to the ${}^{222}Rn_{t+\Delta t} - {}^{222}Rn_t$ term being with the measure uncertainty. To reduce the random errors of the measured ^{222}Rn concentrations, the time window with a width of 1 hour is proposed to smooth the curve (Supplementary information).

Formatted: Superscript

Deleted: 4

3. **Results**

3.1 Time series data

Figure 2 shows the basic climatological parameters of the lake catchment during the campaign month. There are discrete rainfall events occurring throughout the month with an average rainfall of 3.1 mm d^{-1}. The temperature throughout the month ranges from 5.0 – 12.5 ^{o}C within an average of 9.3 ^{o}C. The daily averaged wind speed generally ranges from 0.7 – 2.5 m s^{-1}, with an average of 1.7 m s^{-1}. ^{222}Rn temporal distribution and other time series data are shown in Figure 3a and listed in Supplementary Table 1. Generally, ^{222}Rn concentration varies from 32.2 to 273 Bq m^{-3}, with an average of 144.2 ± 27.7 Bq m^{-3}. ^{222}Rn over the monitoring period shows typical diel cycle, much higher at nighttime and lower in the day time. Figures 3b-3d shows the time series data of temperature (5 mins interval), nearshore lake water level (1 min interval), and wind speed (1 hour interval). Temperature and lake water level also show typical diel cycles, but with antiphase fluctuations with each other. Temperature is higher during the daytime and lower at nighttime. However a sudden decrease of temperature was recorded due to the sudden blizzard (Figure 3b). Water level is higher at nighttime and lower during the daytime, with a strong fluctuation due to the turbulence caused by the blizzard (Figure 3c). The variability might reflect the dynamics of groundwater input and surface water inflow. The air temperature of the lake area is in phase with the water temperature. Wind speed is normally higher during the daytime and lower at nighttime (Figure 3d).

The variation of ^{222}Rn is nearly in antiphase with the fluctuations of lake water temperature and air temperature, indicating that the dominated controlling factors of ^{222}Rn fluctuations are water temperature and wind speed (Figure 3a). This phenomenon is reasonable as lake water ^{222}Rn is predominately lost via atmospheric evasion, which is the function of wind speed and water temperature (Dimova et al. 2015, Dimova and Burnett 2011, Dimova et al. 2013). High water temperature and wind speed leads to elevated atmospheric evasion and causes the decline of ^{222}Rn concentration in the lake water. However, there is a sudden reduction of radon activity from 2: 00 pm to 4: 00 pm on Jul 22nd, 2015, when the snow event led to a sudden decrease of water temperature, increase of wind speed, and large surface water turbulence as indicated by water level fluctuations (Figures 3a-3d). ^{222}Rn in the porewater is 2-3 orders of magnitude larger than ^{222}Rn in the lake water, suggesting that ^{222}Rn is an ideal tracer to estimate the LGD (Supplementary Table 1). ^{222}Rn concentrations in surface water range from 22.2 to 209 Bq m^{-3}, with an average of 92.5 Bq m^{-3} (n = 12), which is in the range of ^{222}Rn continuous monitoring results, suggesting reliable ^{222}Rn measurements (Supplementary Table 2).

3.2 Geochemical results

The results of major ions, nutrients and stable isotopes in different water end members are shown in Figures 4 and 5. Cl^- ranges from 0.6 to 2.1 mg L^{-1} in the surface water (including riverine inflow water, lake water and downstream water), 0.4 to 2.7 mg L^{-1} in porewater and has a much higher concentration of 5.9 mg L^{-1} in rainfall water. Na^{+} ranges from 1.6 to 3.4 mg L^{-1} in the surface water, 1.2 to 4.4 mg L^{-1} in porewater and has a concentration of 4.4 mg L^{-1} in rainfall water. SO_4^{2-} ranges from 1.2 to 2.3 mg L^{-1} in the surface water, 0.4 to 1.7 mg L^{-1} in porewater and has a significant low concentration of 0.01 mg L^{-1} in rainfall water. Ca^{2+} ranges from 3.0 to 12.4 mg L^{-1} in lake water, 3.4 to 12.5 mg L^{-1} in porewater and has a significant high concentration of 20.5 mg L^{-1} in rainfall water. Other concentrations of major ions are listed in Supplementary Table 2. As shown in Figure 4d and Supplementary Table 2, $\delta^{18}O$ in the lake water ranges from - 13.06 ‰ to - 12.11 ‰, with an average of - 12.41 ‰ (n = 7), and $\delta^{2}H$ ranges from - 91.83 ‰ to - 87.47 ‰, with an average of - 89.0 ‰ (n = 7). $\delta^{18}O$ in the riverine inflow water ranges from - 13.44 ‰ to - 13.29 ‰, with an average of – 13.37 ‰ (n = 2), and $\delta^{2}H$ ranges from - 93.25 ‰ to – 91.92 ‰, with an average of - 92.59 ‰ (n = 2). $\delta^{18}O$ in the downstream water ranges from - 12.51 ‰ to - 12.18 ‰, with an average of - 12.35 ‰ (n = 3), and $\delta^{2}H$ ranges from - 88.96 ‰ to - 87.1 ‰, with an average of - 87.98 ‰ (n = 3). $\delta^{18}O$ in the porewater ranges from - 12.66 ‰ to - 11.52 ‰, with an average of - 11.97 ‰ (n = 8), and $\delta^{2}H$ ranges from – 91.3 ‰ to -82.87 ‰, with an average of - 85.5 ‰ (n = 8). DIN in the surface water (including riverine inflow water, lake water and downstream water) range from 6.6 to 16.9 μM, with an average of 10.3 μM, and DIP from 0.36 to 0.41 μM, with an average of 0.38 μM. The concentrations of DIN for the porewater range from 0.7 to 358.8 μM, with an average of 92.8 μM, and DIP from 0.18 to 0.44 μM with an average of 0.31 μM (Figure 5).

4. Discussion

4.1 Proglacial hydrologic processes and geochemical implications

Generally, major ion concentrations in the lake water and porewater of Ximen Co lake are significantly lower than those in main rivers, streams and other tectonic lakes in the QTP (Wang et al. 2010, Wang et al. 2016b, Yao et al. 2015), and are similar to those of snow and glaciers (Liu et al. 2011), suggesting that the lake water is mainly originated from glacier and snow melting. Ion concentrations in the lake and porewater of Ximen Co lake are much lower than those of rainfall collected in Jiuzhi town. This suggests that lake water is less influenced by precipitation (Figures 4a-4c). The concentrations of major ions in the porewater are high compared to the lake water, indicating weathering affects from the aquifer grains. The ratios of Ca^{2+}/Na^{+} in the porewater and groundwater is >1, also suggesting influences of weathering digenesis of major ions from the seasonal frozen ground at the lake shore aquifer (Wang et al. 2010, Weynell et al. 2016, Yao et al. 2015).

The isotopic compositions of the lake water and porewater are significantly isotopic depleted, with values close to the compositions of glaciers and surface snow in the QTP, suggesting the lake is dominantly recharged from snow and glacier melting (Cui et al. 2014, Wang et al. 2016a, Zongxing et al. 2015). The relation of $\delta^{18}O$ versus $\delta^{2}H$ for the lake water is $\delta^{2}H = 4.25 \times \delta^{18}O - 35.99$, with a slope much lower than that of the global meteoric water line (GMWL) (Figure 4d), suggesting the effects of lake surface evaporation. The relation of $\delta^{18}O$ versus $\delta^{2}H$ for the porewater is $\delta^{2}H = 6.93 \times \delta^{18}O - 2.67$, overall on GWML (Figure 4d). Deuterium excesses is defined as $\Delta D = \delta D - 8 \times \delta^{18}O$ (Dansgaard 1964). The value of ΔD is dependent on airmass origins, altitude effect and the kinetic effects during evaporation (Hren et al. 2009). Global meteoric water has a ΔD of + 10 ‰. In the QTP, glacier/snowpack melting water usually has large positive ΔD, while the precipitations derived from warm and humid summer monsoon has lower ΔD (Ren et al. 2017, Ren et al. 2013). In this study, ΔD of surface water, lake and porewater ranges from + 8.5 to + 11.8 ‰, closed to the glacier melting water but much smaller than that of the local precipitation of + 18.8 ‰, This indicates the stream and lake water are mainly originated from glacial/snowpack melting rather than precipitation (Gat 1996, Lerman et al. 1995, Wang et al. 2016a). The slopes of $\delta^{2}H$ versus $\delta^{18}O$ in lake water and porewater are 4.25 and 6.93, both of which are lower than that of GMWL due to

Deleted: 37.1

Deleted: 41.2

Deleted: larger

Deleted: 29.72

Deleted: ^{18}O

surface evaporation. Lake water is more intensively influenced by evaporation compared to porewater. The plots of $\delta^{18}O$ versus Cl^-, and δ^2H versus Cl^- are well clustered for porewater end member (orange area), lake water end member (blue area), riverine inflow water end member (yellow area), and precipitation water (Figures 4e and 4f), suggesting stable $\delta^{18}O$ and δ^2H isotopes and Cl^- can serve as tracers to quantify the hydrologic partitioning of the lake by setting three endmember models.

The concentrations of DIN and DIP are all within the ranges of other glacial melting water and proglacial lake water (Hawkings et al. 2016, Hodson 2007, Hodson et al. 2005, Hudson et al. 2000, Tockner et al. 2002). Briefly, rainfall and upstream lake water such as YN-4 has the highest DIN concentration, indicating the glacier melting and precipitation could be important DIN sources in proglacial areas (Anderson et al. 2017, Dubnick et al. 2017). DIN in porewater is overall higher compared to the lake water, suggesting the porewater to be DIN effective source; and DIP concentrations is higher in the lake water compared to porewater, suggesting the porewater is a DIP sink (Figure 5). The N: P ratios in the lake water and porewater are averaged to be 27.1 and 320.5, respectively, both much larger than the Redfield Ratio (N: P = 16:1) in water and organism in most aquatic system and within the range of other proglacial lakes (Anderson et al. 2017). This also suggests that the lake water and porewater are under phosphate limited condition. N: P ratio in the rainfall water is

30.4, similar to the lake water. The average N: P ratio of porewater is much higher than that of lake water, indicting DIN enrichment in the lake shore aquifers (Figure 5). In pristine groundwater, NO_3^- is the predominated form of N and is highly mobile within the oxic aquifers, leading to much higher DIN concentrations in the porewater; DIP has high affinity to the aquifer grains, resulting in much lower DIP concentrations in the porewater (Lewandowski et al. 2015, Rosenberry et al. 2015, Slomp and Van Cappellen 2004). Thus, in analogous to surface runoff from glacier/snowpack melting, LGD can be also regarded as an important source for the proglacial lakes. Because of very high DIN and N: P ratios in the porewater, a relatively small portion of LGD delivers considerable nutrients into the glacial lake, shifting the aquatic N: P ratios and affecting the proglacial aquatic ecosystem (Anderson et al. 2017).

4.2 Estimation of LGD

Figure 6a shows all the sinks and sources of radon with the epilimnion of the lake. Within ^{222}Rn transient mass balance model, the dominant ^{222}Rn loss is atmospheric degassing/evasion. Generally, ^{222}Rn degassing rate is the function of the radon-222 concentration gradient at the water-air interface and the parameter of gas piston velocity *k*, which is finally the function of wind speed and water temperature (Dimova and Burnett 2011, Gilfedder et al. 2015). To evaluate ^{222}Rn evasion rate, this study employs the widely used method proposed by MacIntyre et al. (1995) which is also detailed described in Supplementary Information. Based on the field data of ^{222}Rn concentration in the lake water, wind speed and temperature log, the radon degassing rate is calculated in a range of 0.8 to 265.2 Bq m^{2} d^{-1}, with an average 42.0 of Bq m^{2} d^{-1}.

In addition to the atmospheric loss and sedimentary diffusion inputs, ^{222}Rn is also sinked via radioactive decay, and sourced from decay of parent isotope of ^{226}Ra. The decay loss of ^{222}Rn fluctuates in phase with the distribution of ^{222}Rn concentration monitored by RAD 7 AQUA. The equations to estimate benthic fluxes are shown in supplementary information. The decay loss is calculated to be 26.4 to 223.4 Bq m^{-2} d^{-1}, with an average of 118.0 $\pm$22.7 Bq m^{-2} d^{-1}. ^{226}Ra concentration is 0.01 Bq m^{-3} for the lake water. Under secular equilibrium, the ^{226}Ra decay input can be calculated by multiplying ^{226}Ra concentration in the lake water with λ_{222} (Corbett et al. 1997, Kluge et al. 2007, Luo et al. 2016). ^{226}Ra decay input is calculated to be 0.83 Bq m^{-2} d^{-1}, which is significantly low compared to other ^{222}Rn sources to the epilimnion.

With the obtained sinks and sources of ^{222}Rn in the lake, and the constants given in Table 1, LGD rate can be obtained by dividing the groundwater derived ^{222}Rn with its concentration in groundwater endmember. The obtained LGD rate, ranges from -23. 7 mm d^{-1} to 90.0 mm d^{-1}, with an average of 10.3 $\pm$8.2 mm d^{-1} (Figure 7) The LGD rate range is relatively less than the daily lake water level variations (≈ 50 mm), indicating that the lake water level variation could be a combined effect of surface runoff and LGD (Hood et al. 2006). The negative values of LGD rate reflect the return groundwater flow due to infiltration into the porewater. Normally, the dominant values are positive, indicating LGD rate is significant compared to water infiltrations into lakeshore aquifer. The temporal variation of LGD rate could be attributed to the fluctuations of the hydraulic gradient in the proglacial areas (Hood et al. 2006, Levy et al. 2015). As indicated by ΔD (mostly > 10) of surface water, the lake and the upstream water is considered to be mainly recharged from glacial/snowpack melting rather other precipitations.

To assess the magnitude of uncertainty of ^{222}Rn transient model, the sensitivity of estimated LGD to changes in other variables is examined. A sensitivity coefficient *f* is proposed to evaluate this uncertainty according to Langston et al. (2013)

$$f = (\Delta F_{LGD} / F_{LGD}) / (\Delta y_i / y_i) \qquad (3)$$

where ΔF_{LGD} is the amount of change in F_{LGD} from the original value. Δy_i is the amount of change in the other variable of y_i from the original value. Thus, higher *f* indicates a large uncertainty of final LGD estimate. The uncertainty mainly stems from ^{222}Rn measurements in different water endmembers, the atmospheric loss and water level record. The uncertainties of ^{222}Rn measurement are about 10 % and 15-20

% in groundwater and lake water endmember, respectively. The uncertainty of atmospheric loss is derived from uncertainty of ^{222}Rn in lake water (with an uncertainty of 15-20 %), temperature (with an uncertainty ≈ 5 %) and wind speed (with an uncertainty ≈ 5 %). Thus, the final LGD estimate has an uncertainty of 35-40 %.

4.3 Hydrologic partitioning

Compared to the groundwater labeled radionuclide of ^{222}Rn, stable $^{18}O/^{2}H$ isotopes are advantageous in the investigation of evaporation processes due to their fractionations from water to vapor and have been widely used to investigate the hydrologic cycle of lakes in various environments (Gat 1995, Gibson et al. 1993, Gonfiantini 1986, Stets et al. 2010). With the field data of stable isotopic composition and Cl^- concentrations in different water end members, groundwater input, surface water input, lake water outflow and infiltration, and evaporation can be partitioned by coupling stable isotopic mass balance model with Cl^- mass balance model (Figure 6b).

The model, consisting of the budgets of stable isotopes and Cl^-, and water masses for the epilimnion, is used to quantify riverine inflow, lake water outflow and infiltration, and evaporation (Gibson et al. 2016, LaBaugh et al. 1995, LaBaugh et al. 1997). The model is valid under the following assumptions: (1) constant density of water; (2) no long-term storage change in the reservoir; (3) well-mixed for the epilimnion (Gibson 2002, Gibson et al. 2016, Gibson and Edwards 2002, LaBaugh et al. 1997). The above assumptions are reasonably tenable during the short monitoring period. The model can be fully expressed as

$$F_{in} + F_{LGD} + F_p = F_E + F_{out} \quad (4)$$

$$F_{in} \times \delta_{in} + F_{LGD} \times \delta_{gw} + F_p \times \delta_p = F_E \times \delta_E + F_{out} \times \delta_L \quad (5)$$

$$F_{in} \times [Cl^-]_{in} + F_{LGD} \times [Cl^-]_{gw} + F_p \times [Cl^-]_p = F_{out} \times [Cl^- \quad (6)$$

where F_{in} [mm d^{-1}] is the surface water inflow to the lake; F_{gw} [mm d^{-1}] is LGD rate. F_p [mm d^{-1}] is the mean daily rainfall rate during the sampling period. F_E [mm d^{-1}] is the lake evaporation. F_{out} [mm d^{-1}] is the lake water outflow via runoff and infiltration into the lake shore aquifer. δ_{in}, δ_{gw},, δ_E and δ_p are the isotopic compositions of surface water inflow, LGD, and evaporative flux, respectively. The values of δ_{in}, δ_{gw},, and δ_p are obtained from field data and the composition of δ_E are cacluated as shown in supplementary information. $[Cl^-]_{in}$, $[Cl^-]_{gw}$, $[Cl^-]_L$ and $[Cl^-]_p$ are the chloride concentrations in the inflow water, porewater, lake water and precipitation, respectively.

The components of the mass balance model can be obtained from the field data of isotopic composition and Cl^- concentrations in different water endmembers. The average ^{18}O composition -13.37 ‰ of riverine inflow water is taken as the value of the input parameter δ_{in}. $\delta^{18}O$ and $\delta^{2}H$ in the groundwater endmember and lake water end member are calculated to be -12.41 ‰ and -87.18 ‰, respectively. $\delta^{18}O$ and $\delta^{2}H$ in the rainfall are measured to be -5.47 ‰ and -24.98 ‰, respectively. With the measured values of δ_L, h, δ_{in}, and the estimated ε and δ_a, the isotopic composition of δ_E is calculated to be -35.11 ‰, which is in line with the results of alpine and arctic lakes elsewhere (Gibson 2002, Gibson et al. 2016, Gibson and Edwards 2002). The values of $[Cl^-]_{in}$, $[Cl^-]_{gw}$, and $[Cl^-]_L$ are calculated to be 0.91 mg L^{-1}, 1.48 mg L^{-1} and 1.02 mg L^{-1}, respectively. All the parameters used in the model are shown in Table 2.

According to Equations 4-6, the uncertainties of calculations of F_{in}, F_{out} and E are mainly derived from the uncertainty of F_{LGD} and the compositions of Cl^-, δD and $\delta^{18}O$ in different water endmembers as suggested in previous studies (Genereux 1998, Klaus and McDonnell 2013). The compositions of Cl^-, δD and $\delta^{18}O$ in surface water, groundwater endmembers have an uncertainty of 5 %. The uncertainty of δ_E is reasonably assumed to be ≈ 20 % . Thus, considering the uncertainty propagation of all the above parameters, the uncertainties of F_{in}, F_{out} and E would be scaled up to 70-80 % of the final estimates.

4.4 The hydrologic partitioning of the glacial lake

Based on the three endmember model of ^{18}O and Cl^-, the riverine inflow rate was calculated to be 135.6 ± 119.0 mm d^{-1}, and the lake outflow rate is estimated to be 141.5 ± 132.4 mm d^{-1}; the evaporation rate is calculated to be 5.2 ± 4.7 mm d^{-1}. The summary of the hydrologic partitioning of the lake is shown in Figure 8a. Generally, the proglacial lake is mostly recharged by the riverine inflow from the snowpack or the glacier melting. The groundwater discharge contributes about only 7.0 % of the total water input to the lake, indicating groundwater input does not dominate water input to the proglacial lake. The recent review on LGD rate by Rosenberry et al. (2015) suggests that the median of LGD rate in the literatures is 7.4 mm d^{-1} (0.05 mm d^{-1} to 133 mm d^{-1}), which is about 2/3 of LGD rate in this study. This difference may be due to the hydrogeological setting of the lake shore aquifer. This aquifer is formed by grey loam, clayey soil and sand (Lehmkuhl 1998, Schlutz and Lehmkuhl 2009), which is with relatively high permeability. Previous studies have indicated that groundwater forms a key component of proglacial hydrology (Levy et al. 2015). However, there have been limited quantitative studies of groundwater contribution to hydrologic budget of proglacial areas. This study further summarizes the groundwater discharge studies over the glacial forefield areas. Based on long term hydrological and climatological parameter monitoring on the Nam Co lake in the QTP, Zhou et al. (2013) estimated the LGD to be 5-8 mm d^{-1} , which is comparable to the surface

Deleted: The lake water is mainly lost v surface water outflow and infiltration to lake shore aquifers. The evaporation constitutes relatively small ratio (≈ 3.5 of total water losses. The annual evaporation rate was recorded to be 142 mm (equivalent to 3.92 mm d^{-1}) in 2015 the Jiuzhi weather station, lower than th obtained evaporation in this study. This may be due to much higher evaporation August during the monitoring period.

Formatted: Font color: Red

Formatted: Font color: Red

Deleted: Brown et al. (2006), (Zhou e 2013)

Formatted: Superscript

runoff input and LGD of this study. Brown et al. (2006) investigated the headwater streams at the proglacial areas of Taillon Glacier in French and found that groundwater contributes 6-10 % of the stream water immediate downwards of the glacier. Using water mass balance model, Hood et al. (2006) shows that groundwater inflow is substantial in the hydrologic partitioning of the proglacial Lake O'Hara in front of Opabin Glacier in Canada and comprised of 30 -74 % of the total inflow. Roy and Hayashi (2008) studied the proglacial lakes of Hungabee lake and Opabin lake at glacier forefield of Opabin Glacier and found that groundwater component is predominant water sources of the lakes and consisted of 35-39 % of the total water input of the lakes. Langston et al. (2013) further investigated a tarn immediate in front of Opabin Glacier and indicated the tarn is predominantly controlled by groundwater inflow/outflow, which consisted of 50-100 % of total tarn volume. Magnusson et al. (2014) studied the streams in the glacier forefield of Dammagletscher, Switzerland and revealed that groundwater contributed only 1-8 % of the total surface runoff. Groundwater contribution in this study is similar to those obtained the mountainous proglacial areas in Europe, but much lower than those obtained in the proglacial areas of polar regions. It is concluded that proglacial lakes/streams in front of mountainous glaciers are mainly recharged by surface runoff from glacier/snowpack melting. This might be due to well-developed stream networks and limited deep groundwater flow

(Brown et al. 2006, Einarsdottir et al. 2017, Magnusson et al. 2014). However, proglacial tarns and lakes in the polar areas are predominantly controlled by groundwater discharge, due to less connectivity of surface runoff and high shallow and deep groundwater connectivity (Hood et al. 2006, Langston et al. 2013, Roy and Hayashi 2008).

The evaporation constitutes relatively small ratio (≈ 3.5 %) of total water losses. The annual evaporation rate was recorded to be 1429.8 mm (equivalent to 3.92 mm d^{-1}) in 2015 by the Jiuzhi weather station, lower than the obtained evaporation in this study. This may be due to much higher evaporation in August during the monitoring period. The estimation of evaporation in this study generally represents the upper limit of the lake, as the sampling campaign was conducted during the summer time when the highest evaporation might occur. The lake surface evaporation derived from the pan evaporation in the QTP ranges from ~ 700 mm yr^{-1} in the eastern QTP to over 1400 mm yr^{-1} in the interior lakes of the QTP (Ma et al. 2015, Yang et al. 2014, Zhang et al. 2007). The evaporation of this study is rather in line with the previous evaporation observation in the eastern QTP, stressing the tenability of evaporation in this study. The runoff input is predominated recharge component (> 90 %) compared to other components, with an area normalized value comparable to previous studies of runoff input in other glacial melting dominant lakes in the QTP (Biskop et al. 2016, Zhang et

Deleted: The lake water is mainly lost v surface water outflow and infiltration to lake shore aquifers.

Formatted: Indent: First line: 0 ch

Deleted: ese studies

Deleted: s

Deleted: Eastern QTP

Deleted: is

Deleted: over

Deleted: ≈

Formatted: Superscript

Formatted: Superscript

Deleted: e

al. 2011, Zhou et al. 2013). The runoff input and the lake evaporation of the study area, however, are subject to highly daily, seasonal and inter-annual variability as indicated by previous studies in the QTP (Lazhu et al. 2016, Lei et al. 2017, Ma et al. 2015, Zhou et al. 2013). Therefore, further investigations of long term and high resolution climatological and isotopic data are required to provide precise constraints of hydrologic partitioning of the lakes in the QTP.

4.5 LGD derived nutrient loadings, nutrient budget and ecological implications

Compared to extensive studies of SGD derived nutrient loadings in the past decade (Luo and Jiao 2016, Slomp and Van Cappellen 2004), studies of LGD derived nutrient loadings have received limited attention, even given the fact that groundwater in lake shore aquifers is usually concentrated in nutrients (Lewandowski et al. 2015, Rosenberry et al. 2015). Even fewer studies focus on chemical budgets in the proglacial lakes which are often difficult to access for sampling. Groundwater borne DIN and DIP across the sediment-water interface in this study are determined with an equation coupling the advective or LGD-derived, and diffusive solute transport (Hagerthey and Kerfoot 1998, Lerman et al. 1995)

$$F_j = -nD_j^m \frac{dC_j}{dx} + v_{gw} C_j \quad (7)$$

where $-nD_j^m \frac{dC_j}{dx}$ is the diffusion input and $v_{gw} C_j$ is the LGD derived fluxes, F_j

Deleted: es

Deleted: (Ma et al. 2015, Zhang et al. 2007)(Zhang et al. 2013)

Formatted: Font color: Red

Deleted: .

[μM m^{-2} d^{-1}] is the mol flux of nutrient species *j* (representing DIN or DIP). *n* is the sediment porosity. D_j^m is the molecular diffusion coefficient of nutrient species *j*, which is given to be 4.8 x 10^{-5} m^2 d^{-1} for DIP (Quigley and Robbins 1986), and 8.8 x 10^{-5} m^2 d^{-1} for DIN (Li and Gregory 1974), respectively. C_j [μM] is the concentration of nutrient species *j*. *x*[m] is the sampling depth. v_{gw} is LGD rate estimated by ^{222}Rn mass balance model and has a value of 10.3 $\pm$8.2 mm d^{-1}. $\frac{dC_j}{dx}$ is the concentration gradient of nutrient species *j* across the water-sedimentary interface.

Substituting the constants and the field data of DIN and DIP in to Equation 6, LGD derived nutrient loadings are calculated to be 954.3 μmol m^{-2} d^{-1} and 3.2 μmol m^{-2} d^{-1} for DIN and DIP, respectively. Riverine inflow brings 1195.0 μmol m^{-2} d^{-1} DIN, 52.9 μmol m^{-2} d^{-1} DIP into the lake. Lake water outflow derived nutrient loss is estimated to be 1439.9 μmol m^{-2} d^{-1} and 54.7 μmol m^{-2} d^{-1} for DIN and DIP, respectively. Nutrients in the lake can be also sourced from atmospheric deposit (mostly in form of precipitation). With the nutrient concentrations in the rain water during the monitoring period, the wet deposit is calculated to be 76 μmol m^{-2} d^{-1} and 2.5 μmol m^{-2} d^{-1}, for DIN and DIP, respectively. The loadings of DIN to the lakes are mainly from surface runoff and LGD, which comprised of 42.9 % and 53.7 % of the total DIN loadings. Groundwater derived DIP input, however, constitutes only 6.3 % of the total DIP inputs to the lake, indicating groundwater borne DIP is less contributive to the

Deleted: ..

nutrient budget of the lake compared to DIN. Very recent studies on polar regions have indicated that the glacier/snowpack water is the main N sources to the proglacial lakes (Anderson et al. 2013, Dubnick et al. 2017). However, they do not consider the contribution of groundwater borne N, in spite of the high groundwater connectivity in the proglacial areas (Roy and Hayashi 2008). This study stresses that groundwater borne DIN could be comparable to the surface runoff derived DIN.

Based on nutrient results, the lake is considered to be an oligotrophic lake, similar to other glacier melting dominant lakes in the QTP (Liu et al. 2011, Mitamura et al. 2003). Phytoplankton is good dissolved organic phosphate (DOP) recyclers and will overcome inorganic P limitation though DOP cycling in most template lakes (Hudson et al. 2000). However, this may be not applicable for the glacial melting water and the peri/pro-glacial lake water. Previous studies show that phosphate nutrients are dominated by DIP and particulate phosphate, and the DOP contributes less than 10 % of the dissolved phosphate (Cole et al. 1998, Hawkings et al. 2016, Hodson 2007). Thus DOP recycling is not likely to low N: P ratio under these conditions. Thus, the primary production (PP) is therefore considered to be controlled by the DIP loadings. The sum of DIN and DIP inputs minus the calculated DIN and DIP outputs leads to surpluses of 785.4 μmol m^{-2} d^{-1} and 3.9 μmol m^{-2} d^{-1} for DIN and DIP, respectively. The surpluses are expected to be consumed by the phytoplankton and converted into

Deleted: elsewhere

Deleted: and under phosphate limited condition

Moved down [1]: Thus, the primary production (PP) is therefore considered t be controlled by the DIP loadings. The s of DIN and DIP inputs minus the sum of calculated DIN and DIP outputs leads to surpluses of 785.4 μmol m^{-2} d^{-1} and 3.9 μmol m^{-2} d^{-1} for DIN and DIP, respective

Deleted: d

Field Code Changed

Deleted: ?

Deleted: ?

Deleted: is?

Field Code Changed

Deleted: are

Deleted: er

Deleted: The surpluses are expected to consumed by the phytoplankton and converted into the PP under the Red Fiel ratio (C: N: P = 106: 16: 1), leading to a of 0.41 mmol C m^{-2} d^{-1}.

Moved (insertion) [1]

Deleted: ?

Deleted: difference between the

Deleted: sum of

Deleted: and

Deleted: minus

Deleted: sum of the

the PP under phosphate limited conditions. As primary producers in the fresh lacustrine system consume the nutrient under variant N: P ratios (7.1 to 44.2, mean: 22.9) (Downing and McCauley 1992), the biological uptake of DIN is roughly estimated to be 89.3 $\mu M\ m^{2}\ d^{-1}$. Therefore, the nutrient budgets for DIN and DIP can be finally conceptualized in Figures 8b and 8c.

4.6. Implications, prospective and limitations

Mountainous proglacial lakes are readily developed in glacier forefields of QTP and other high mountainous glacial such as Europe Alps and Pamir at central Asian (Heckmann et al. 2016). The proglacial lakes are always trapping system of sediment and sinks for water and chemical originated from glacier/snowpack melting and groundwater. In analogous to cosmogenic isotopes such as ^{10}Be serving as a tool to quantify the sediment sources, approaches integrating ^{222}Rn and stable isotopes provides both qualitatively and quantitatively evaluations of groundwater contributions and hydrologic partitioning in these remote and untapped lacustrine systems. Thus, it is expected that the multiple aqueous isotopes is considered to be effective tools to investigate the LGD and hydrologic partitioning in other proglacial lakes. This study is mainly limited by the relatively short sampling and monitoring period. As a special hydrologic regime, the lake shore aquifers of the proglacial lakes are experiencing frozen-unfrozen transition seasonally, and the dominant recharge of

Field Code Changed

Formatted: Superscript

Deleted: The

Formatted: Font: Times New Roman

Formatted: Superscript

Deleted: are

Deleted: as summarized

Deleted: The estimated primary productivity is lower than most temperat eutrophicated and ologotrophic lakes (C et al. 1998, Smith 1979), and comparabl some high latitude or altitude lakes (Richerson et al. 1986, Sterner 2010).

glacial melting could be fluctuated significantly due to air temperature variation. Therefore, future groundwater and hydrological studies can be extended to longtime sampling and monitoring of stable isotopes and ^{222}Rn in different water endmembers to reveal the seasonally hydrological and hydrogeological dynamics and their impacts on local biogeochemical cycles and ecological systems. Special concerns would be placed on how surface/groundwater interactions and the associated biogeochemical processes in response to the seasonal frozen ground variations and glacier/snowpack melting intensity.

Deleted: .

5. Conclusion

Deleted:

A ^{222}Rn continuous monitoring is conducted at Ximen Co Lake, a proglacial lake located at the east QTP. A dynamic ^{222}Rn mass balance model constrained by radium mass balance and water level fluctuation is used to quantify temporal distribution of LGD of the lake. The obtained LGD over the monitoring time ranges from – 23. 7 mm d^{-1} to 80.9 mm d^{-1}, with an average of 10.3 ± 8.2 mm d^{-1}. Thereafter, a three endmember model consisting of the budgets of water, stable isotopes and Cl^- is used to depict the hydrologic partitioning of the lake. Riverine inflow, lake water outflow via surface runoff, and surface evaporation are estimated to be 135.6 mm d^{-1}, 141.5 mm d^{-1} and 5.2 mm d^{-1}, respectively. LGD derived nutrient loading is estimated to be

785.4 μmol m^{-2} d^{-1} and 3.2 μmol m^{-2} d^{-1} for DIN and DIP, respectively. This study also implicates that LGD constitutes relatively small portion of the proglacial hydrologic partitioning, however, delivers nearly a half of the nutrient loadings to the proglacial lake.

This study presents the first attempt to quantify LGD and the associated nutrient loadings to the proglacial lake of QTP. To our knowledge, there is almost no study on the groundwater-lake water interaction in the high altitude proglacial lakes in QTP. This study demonstrates that ^{222}Rn based approach can be used to investigate the groundwater dynamics in the high altitude proglacial lakes. The method is instructional to similar studies in other proglacial lakes in the QTP and elsewhere. For a comprehensive understanding the hydrological and biogeochemical dynamics in the QTP, interdisciplinary and multi-approach integrated studies are in great need. Of particular importance are the lake hydrology and groundwater surface water interaction studies based on multiple approaches such as remote sensing products, long term and high resolution observation of climatological parameters and isotopic data.

Acknowledgements

This study was supported by grants from the National Natural Science Foundation of

Deleted: Upon depicting nutrient budg within the lake, the primary productivity estimated to be 0.41 mol C m^{-2} d^{-1}.

Deleted: international,

Deleted: ,

Deleted: ,

Deleted: based constraining and numerical modeling

Deleted: .

China (NSFC, No.41572208) and (NSFC, 91747204), and the Research Grants Council of Hong Kong Special Administrative Region, China (HKU17304815). The authors thank Mr. Buming Jiang for his kind help in the field works during the campaign and Ergang Lian for his help in stable isotope analysis. The authors thank Jessie Lai for her help in FIA analysis in School of Biological Sciences, HKU. Supporting data are included as in the files of supplementary information 2 and 3; Climatological data are purchased through http://www.weatherdt.com/shop.html; any additional data may be obtained from L.X. (email: xinluo@hku.hk);

References

Åberg, J., Jansson, M. and Jonsson, A. (2010) Importance of water temperature and thermal stratification dynamics for temporal variation of surface water CO_2 in a boreal lake. Journal of Geophysical Research: Biogeosciences (2005–2012) 115(G2).

Andermann, C., Longuevergne, L., Bonnet, S., Crave, A., Davy, P. and Gloaguen, R. (2012) Impact of transient groundwater storage on the discharge of Himalayan rivers. Nature Geoscience 5(2), 127-132.

Anderson, L., Birks, J., Rover, J. and Guldager, N. (2013) Controls on recent Alaskan lake changes identified from water isotopes and remote sensing. Geophysical Research Letters 40(13), 3413-3418.

Anderson, N.J., Saros, J.E., Bullard, J.E., Cahoon, S.M., McGowan, S., Bagshaw, E.A., Barry, C.D., Bindler, R., Burpee, B.T. and Carrivick, J.L. (2017) The Arctic in the Twenty-First Century: Changing Biogeochemical Linkages across a Paraglacial Landscape of Greenland. BioScience 67(2), 118-133.

Barry, R.G. (2006) The status of research on glaciers and global glacier recession: a review. Progress in Physical Geography 30(3), 285-306.

Batlle-Aguilar, J., Harrington, G.A., Leblanc, M., Welch, C. and Cook, P.G. (2014) Chemistry of groundwater discharge inferred from longitudinal river sampling. Water Resources Research 50(2), 1550-1568.

Belanger, T.V., Mikutel, D.F. and Churchill, P.A. (1985) Groundwater seepage nutrient loading in a Florida Lake. Water Research 19(6), 773-781.

Biskop, S., Maussion, F., Krause, P. and Fink, M. (2016) Differences in the water-balance components of four lakes in the southern-central Tibetan Plateau. Hydrology and Earth System Sciences 20(1), 209.

Blume, T., Krause, S., Meinikmann, K. and Lewandowski, J. (2013) Upscaling lacustrine groundwater discharge rates by fiber-optic distributed temperature sensing. Water Resources Research 49(12), 7929-7944.

Böhner, J. (1996) Säkulare Klimaschwankungen und rezente Klimatrends Zentral-und Hochasiens, Goltze.

Böhner, J. (2006) General climatic controls and topoclimatic variations in Central and High Asia. Boreas 35(2), 279-295.

Bolch, T., Kulkarni, A., Kääb, A., Huggel, C., Paul, F., Cogley, J.G., Frey, H., Kargel, J.S., Fujita, K., Scheel, M., Bajracharya, S. and Stoffel, M. (2012) The State and Fate of Himalayan Glaciers. Science 336(6079), 310-314.

Brown, L.E., Hannah, D.M., Milner, A.M., Soulsby, C., Hodson, A.J. and Brewer, M.J. (2006) Water source dynamics in a glacierized alpine river basin (Taillon-Gabiétous, French Pyrénées). Water Resources Research 42(8).

Burnett, W.C., Peterson, R.N., Santos, I.R. and Hicks, R.W. (2010) Use of automated radon measurements for rapid assessment of groundwater flow into Florida streams. Journal of Hydrology 380(3), 298-304.

Callegary, J.B., Kikuchi, C.P., Koch, J.C., Lilly, M.R. and Leake, S.A. (2013) Review: Groundwater in Alaska (USA). Hydrogeology Journal 21(1), 25-39.

Cole, J., Nina, J. and Caraco, F. (1998) Atmospheric exchange of carbon dioxide in a low-wind oligotrophic lake measured by the addition of SF_6. Limnology and Oceanography 43, 647-656.

Cook, P., Lamontagne, S., Berhane, D. and Clark, J. (2006) Quantifying groundwater discharge to Cockburn River, southeastern Australia, using dissolved gas tracers 222Rn and SF6. Water Resources Research 42(10).

Cook, P.G., Favreau, G., Dighton, J.C. and Tickell, S. (2003) Determining natural groundwater influx to a tropical river using radon, chlorofluorocarbons and ionic environmental tracers. Journal of Hydrology 277(1–2), 74-88.

Corbett, D.R., Burnett, W.C., Cable, P.H. and Clark, S.B. (1997) Radon tracing of groundwater input into Par Pond, Savannah River site. Journal of Hydrology 203(1), 209-227.

Cui, X., Ren, J., Qin, X., Sun, W., Yu, G., Wang, Z. and Liu, W. (2014) Chemical characteristics and environmental records of a snow-pit at the Glacier No. 12 in the Laohugou Valley, Qilian Mountains. Journal of Earth Science 25(2), 379-385.

Dansgaard, W. (1964) Stable isotopes in precipitation. Tellus A 16(4).

Dimova, N., Paytan, A., Kessler, J.D., Sparrow, K., Garcia-Tigreros Kodovska, F., Lecher, A.L., Murray, J. and Tulaczyk, S.M. (2015) The current magnitude and mechanisms of groundwater discharge in the Arctic: a case study from Alaska. Environmental Science & Technology 49(20), 12036-12043.

Dimova, N.T. and Burnett, W.C. (2011) Evaluation of groundwater discharge into small lakes based on the temporal distribution of radon-222. Limnol. Oceanogr 56(2), 486-494.

Dimova, N.T., Burnett, W.C., Chanton, J.P. and Corbett, J.E. (2013) Application of radon-222 to investigate groundwater discharge into small shallow lakes. Journal of Hydrology 486, 112-122.

Downing, J.A. and McCauley, E. (1992) The nitrogen: phosphorus relationship in lakes. Limnology and Oceanography 37(5), 936-945.

Dubnick, A., Wadham, J., Tranter, M., Sharp, M., Orwin, J., Barker, J., Bagshaw, E. and Fitzsimons, S. (2017) Trickle or treat: The dynamics of nutrient export from polar glaciers. Hydrological Processes 31(9), 1776-1789.

Einarsdottir, K., Wallin, M.B. and Sobek, S. (2017) High terrestrial carbon load via groundwater to a boreal lake dominated by surface water inflow. Journal of Geophysical Research: Biogeosciences 122(1), 15-29.

Farinotti, D., Longuevergne, L., Moholdt, G., Duethmann, D., Molg, T., Bolch, T., Vorogushyn, S. and Guntner, A. (2015) Substantial glacier mass loss in the Tien Shan over the past 50 years. Nature Geosci 8(9), 716-722.

Gat, J. (1995) Physics and chemistry of lakes, pp. 139-165, Springer.

Gat, J. (1996) Oxygen and hydrogen isotopes in the hydrologic cycle. Annual Review of Earth and Planetary Sciences 24(1), 225-262.

Genereux, D. (1998) Quantifying uncertainty in tracer-based hydrograph separations. Water Resources Research 34(4), 915-919.

Gibson, J., Edwards, T., Bursey, G. and Prowse, T. (1993) Estimating evaporation using stable isotopes: quantitative results and sensitivity analysis for. Nordic Hydrology 24, 79-94.

Gibson, J.J. (2002) Short-term evaporation and water budget comparisons in shallow Arctic lakes using non-steady isotope mass balance. Journal of Hydrology 264(1), 242-261.

Gibson, J.J., Birks, S.J. and Yi, Y. (2016) Stable isotope mass balance of lakes: a contemporary perspective. Quaternary Science Reviews 131, Part B, 316-328.

Gibson, J.J. and Edwards, T.W.D. (2002) Regional water balance trends and evaporation-transpiration partitioning from a stable isotope survey of lakes in northern Canada. Global Biogeochemical Cycles 16(2), 10-11-10-14.

Gilfedder, B., Frei, S., Hofmann, H. and Cartwright, I. (2015) Groundwater discharge to wetlands driven by storm and flood events: Quantification using continuous Radon-222 and electrical conductivity measurements and dynamic mass-balance modelling. Geochimica Et Cosmochimica Acta 165, 161-177.

Gonfiantini, R. (1986) Environmental isotopes in lake studies. Handbook of environmental isotope geochemistry 2, 113-168.

Good, S.P., Noone, D. and Bowen, G. (2015) Hydrologic connectivity constrains partitioning of global terrestrial water fluxes. Science 349(6244), 175-177.

Hagerthey, S.E. and Kerfoot, W.C. (1998) Groundwater flow influences the biomass and nutrient ratios of epibenthic algae in a north temperate seepage lake. Limnology and Oceanography 43(6), 1227-1242.

Harris, C., Arenson, L.U., Christiansen, H.H., Etzelmüller, B., Frauenfelder, R., Gruber, S., Haeberli, W., Hauck, C., Hölzle, M. and Humlum, O. (2009) Permafrost and climate in Europe: Monitoring and modelling thermal, geomorphological and geotechnical responses. Earth-Science Reviews 92(3), 117-171.

Hasler, C.T., Midway, S.R., Jeffrey, J.D., Tix, J.A., Sullivan, C. and Suski, C.D. (2016) Exposure to elevated pCO_2 alters post-treatment diel movement patterns of largemouth bass over short time scales. Freshwater Biology 61(9), 1590-1600.

Hawkings, J., Wadham, J., Tranter, M., Telling, J., Bagshaw, E., Beaton, A., Simmons, S.L., Chandler, D., Tedstone, A. and Nienow, P. (2016) The Greenland Ice Sheet as a hot spot of phosphorus weathering and export in the Arctic. Global Biogeochemical Cycles, 30(2), 191-210.

Heckmann, T., McColl, S. and Morche, D. (2015) Retreating ice: research in pro-glacial areas matters. Earth Surface Processes and Landforms, 41(2), 271-276.

Heckmann, T., McColl, S. and Morche, D. (2016) Retreating ice: research in pro-glacial areas matters. Earth Surface Processes and Landforms 41(2), 271-276.

Hodson, A. (2007) Phosphorus in glacial meltwaters. Glacier Science and Environmental Change, 81-82.

Hodson, A., Mumford, P., Kohler, J. and Wynn, P.M. (2005) The High Arctic glacial ecosystem: new insights from nutrient budgets. Biogeochemistry 72(2), 233-256.

Hood, J.L., Roy, J.W. and Hayashi, M. (2006) Importance of groundwater in the water balance of an alpine headwater lake. Geophysical Research Letters 33(13).

Hren, M.T., Bookhagen, B., Blisniuk, P.M., Booth, A.L. and Chamberlain, C.P. (2009) $\delta^{18}O$ and δD of streamwaters across the Himalaya and Tibetan Plateau: Implications for moisture sources and paleoelevation reconstructions. Earth and Planetary Science Letters 288(1), 20-32.

Hudson, J.J., Taylor, W.D. and Schindler, D.W. (2000) Phosphate concentrations in lakes. Nature 406(6791), 54-56.

Johannes, R.E. (1980) The Ecological Significance of the Submarine Discharge of Groundwater. Marine Ecology-Progress Series 3(4), 365-373.

Kim, G., Burnett, W.C., Dulaiova, H., Swarzenski, P.W. and Moore, W.S. (2001) Measurement of Ra-224 and Ra-226 activities in natural waters using a radon-in-air monitor. Environmental Science & Technology 35(23), 4680-4683.

Klaus, J. and McDonnell, J. (2013) Hydrograph separation using stable isotopes: Review and evaluation. Journal of Hydrology 505, 47-64.

Kluge, T., Ilmberger, J., Rohden, C.v. and Aeschbach-Hertig, W. (2007) Tracing and quantifying groundwater inflow into lakes using a simple method for radon-222 analysis. Hydrology and Earth System Sciences 11(5), 1621-1631.

Kluge, T., von Rohden, C., Sonntag, P., Lorenz, S., Wieser, M., Aeschbach-Hertig, W. and Ilmberger, J. (2012) Localising and quantifying groundwater inflow into lakes using high-precision ^{222}Rn profiles. Journal of Hydrology 450, 70-81.

Kraemer, T.F. (2005) Radium isotopes in Cayuga Lake, New York: Indicators of inflow and mixing processes. Limnology and Oceanography 50(1), 158-168.

LaBaugh, J.W., Rosenberry, D.O. and Winter, T.C. (1995) Groundwater contribution to the water and chemical budgets of Williams Lake, Minnesota, 1980-1991. Canadian Journal of Fisheries and Aquatic Sciences 52(4), 754-767.

LaBaugh, J.W., Winter, T.C., Rosenberry, D.O., Schuster, P.F., Reddy, M.M. and Aiken, G.R. (1997) Hydrological and chemical estimates of the water balance of a closed-basin lake in north central Minnesota. Water Resources Research 33(12), 2799-2812.

Langston, G., Hayashi, M. and Roy, J.W. (2013) Quantifying groundwater-surface water interactions in a proglacial moraine using heat and solute tracers. Water Resources Research 49(9), 5411-5426.

Lazar, B., Weinstein, Y., Paytan, A., Magal, E., Bruce, D. and Kolodny, Y. (2008) Ra and Th adsorption coefficients in lakes—Lake Kinneret (Sea of Galilee)“natural experiment”. Geochimica Et Cosmochimica Acta 72(14), 3446-3459.

Lazhu, Yang, K., Wang, J., Lei, Y., Chen, Y., Zhu, L., Ding, B. and Qin, J. (2016) Quantifying evaporation and its decadal change for Lake Nam Co, central Tibetan Plateau. Journal of Geophysical Research (Atmospheres) 121, 7578-7591.

Lecher, A.L., Kessler, J., Sparrow, K., Garcia-Tigreros Kodovska, F., Dimova, N., Murray, J., Tulaczyk, S. and Paytan, A. (2015) Methane transport through submarine groundwater discharge to the North Pacific and Arctic Ocean at two Alaskan sites. Limnology and Oceanography, 61(S1).

Lee, C.M., Jiao, J.J., Luo, X. and Moore, W.S. (2012) Estimation of submarine groundwater discharge and associated nutrient fluxes in Tolo Harbour, Hong Kong. Science of the Total Environment 433, 427-433.

Lee, D.R. (1977) A device for measuring seepage flux in lakes and estuaries.

Limnology and Oceanography 22(1), 140-147.

Lee, D.R., Cherry, J.A. and Pickens, J.F. (1980) Groundwater transport of a salt tracer through a sandy lakebed. Limnology and Oceanography 25(1), 45-61.

Lehmkuhl, F. (1998) Extent and spatial distribution of Pleistocene glaciations in eastern Tibet. Quaternary International 45–46, 123-134.

Lei, Y., Yao, T., Yang, K., Sheng, Y., Kleinherenbrink, M., Yi, S., Bird, B.W., Zhang, X., Zhu, L. and Zhang, G. (2017) Lake seasonality across the Tibetan Plateau and their varying relationship with regional mass changes and local hydrology. Geophysical Research Letters 44(2), 892-900.

Lemieux, J.M., Sudicky, E.A., Peltier, W.R. and Tarasov, L. (2008a) Dynamics of groundwater recharge and seepage over the Canadian landscape during the Wisconsinian glaciation. Journal of Geophysical Research: Earth Surface (2003–2012) 113(F1).

Lemieux, J.M., Sudicky, E.A., Peltier, W.R. and Tarasov, L. (2008b) Simulating the impact of glaciations on continental groundwater flow systems: 1. Relevant processes and model formulation. Journal of Geophysical Research: Earth Surface 113(F3), n/a-n/a.

Lemieux, J.M., Sudicky, E.A., Peltier, W.R. and Tarasov, L. (2008c) Simulating the impact of glaciations on continental groundwater flow systems: 2. Model application to the Wisconsinian glaciation over the Canadian landscape. Journal of Geophysical Research: Earth Surface (2003–2012) 113(F3).

Lerman, A., Imboden, D. and Gat, J. (1995) Physics and chemistry of lakes. New York.

Levy, A., Robinson, Z., Krause, S., Waller, R. and Weatherill, J. (2015) Long-term variability of proglacial groundwater-fed hydrological systems in an area of glacier retreat, Skeiðarársandur, Iceland. Earth Surface Processes and Landforms 40(7), 981-994.

Lewandowski, J., Meinikmann, K., Nützmann, G. and Rosenberry, D.O. (2015) Groundwater – the disregarded component in lake water and nutrient budgets. Part 2: effects of groundwater on nutrients. Hydrological Processes 29(13), 2922-2955.

Lewandowski, J., Meinikmann, K., Ruhtz, T., Pöschke, F. and Kirillin, G. (2013) Localization of lacustrine groundwater discharge (LGD) by airborne measurement of thermal infrared radiation. Remote Sensing of Environment 138, 119-125.

Li, Y.H. and Gregory, S. (1974) Diffusion of Ions in Sea-Water and in Deep-Sea Sediments. Geochimica Et Cosmochimica Acta 38(5), 703-714.

Liu, C., Liu, J., Wang, X.S. and Zheng, C. (2015) Analysis of groundwater–lake interaction by distributed temperature sensing in Badain Jaran Desert, Northwest China. Hydrological Processes 30(9), 1330-1341.

Liu, Y., Yao, T., Jiao, N., Tian, L., Hu, A., Yu, W. and Li, S. (2011) Microbial diversity in the snow, a moraine lake and a stream in Himalayan glacier. Extremophiles 15(3), 411-421.

Luo, X. and Jiao, J.J. (2016) Submarine groundwater discharge and nutrient loadings in Tolo Harbor, Hong Kong using multiple geotracer-based models, and their implications of red tide outbreaks. Water Research 102, 11-31.

Luo, X., Jiao, J.J., Liu, Y., Zhang, X., Liang, W. and Tang, D. (2018) Evaluation of Water Residence Time, Submarine Groundwater Discharge, and Maximum New Production Supported by Groundwater Borne Nutrients in a Coastal Upwelling Shelf System. Journal of Geophysical Research: Oceans 123(1), 631-655.

Luo, X., Jiao, J.J., Moore, W. and Lee, C.M. (2014) Submarine groundwater discharge estimation in an urbanized embayment in Hong Kong via short-lived radium isotopes and its implication of nutrient loadings and primary production. Marine Pollution Bulletin 82(1), 144-154.

Luo, X., Jiao, J.J., Wang, X.-s. and Liu, K. (2016) Temporal ^{222}Rn distributions to reveal groundwater discharge into desert lakes: implication of water balance in the Badain Jaran Desert, China. Journal of Hydrology 534, 87-103.

Luo, X., Jiao, J.J., Wang, X.-s., Liu, K., Lian, E. and Yang, S. (2017) Groundwater discharge and hydrologic partition of the lakes in desert environment: Insights from stable ^{18}O/^{2}H and radium isotopes. Journal of Hydrology 546, 189-203.

Ma, N., Zhang, Y., Szilagyi, J., Guo, Y., Zhai, J. and Gao, H. (2015) Evaluating the complementary relationship of evapotranspiration in the alpine steppe of the Tibetan Plateau. Water Resources Research 51(2), 1069-1083.

MacIntyre, S., Wannikhof, R., Chanton, J.P., Matson, P.A. and Hariss, R.C. (1995) Biogenic Trace Gases: Measuring Emissions from Soil and Water.

Magnusson, J., Kobierska, F., Huxol, S., Hayashi, M., Jonas, T. and Kirchner, J.W. (2014) Melt water driven stream and groundwater stage fluctuations on a glacier forefield (Dammagletscher, Switzerland). Hydrological Processes 28(3), 823-836.

Mitamura, O., Seike, Y., Kondo, K., Goto, N., Anbutsu, K., Akatsuka, T., Kihira, M., Tsering, T.Q. and Nishimura, M. (2003) First investigation of ultraoligotrophic alpine Lake Puma Yumco in the pre-Himalayas, China. Limnology 4(3), 167-175.

Moore, W.S. (1976) Sampling radium-228 in the deep ocean. Deep Sea Res. 23, 647-651.

Nakayama, T. and Watanabe, M. (2008) Missing role of groundwater in water and nutrient cycles in the shallow eutrophic Lake Kasumigaura, Japan. Hydrological Processes 22(8), 1150-1172.

Paytan, A., Lecher, A.L., Dimova, N., Sparrow, K.J., Kodovska, F.G.-T., Murray, J., Tulaczyk, S. and Kessler, J.D. (2015) Methane transport from the active layer to lakes in the Arctic using Toolik Lake, Alaska, as a case study. Proceedings of the National

Academy of Sciences 112(12), 3636-3640.

Qiu, J. (2008) China: the third pole. Nature News 454(7203), 393-396.

Quigley, M.A. and Robbins, J.A. (1986) Phosphorus release processes in nearshore southern Lake Michigan. Canadian Journal of Fisheries and Aquatic Sciences 43(6), 1201-1207.

Ren, W., Yao, T., Xie, S. and He, Y. (2017) Controls on the stable isotopes in precipitation and surface waters across the southeastern Tibetan Plateau. Journal of Hydrology 545, 276-287.

Ren, W., Yao, T., Yang, X. and Joswiak, D.R. (2013) Implications of variations in δ18O and δD in precipitation at Madoi in the eastern Tibetan Plateau. Quaternary International 313–314, 56-61.

Rosenberry, D.O., Lewandowski, J., Meinikmann, K. and Nützmann, G. (2015) Groundwater-the disregarded component in lake water and nutrient budgets. Part 1: effects of groundwater on hydrology. Hydrological Processes 29(13), 2895-2921.

Roy, J.W. and Hayashi, M. (2008) Groundwater exchange with two small alpine lakes in the Canadian Rockies. Hydrological Processes 22(15), 2838-2846.

Schafran, G.C. and Driscoll, C.T. (1993) Flow path-composition relationships for groundwater entering an acidic lake. Water Resources Research 29(1), 145-154.

Scheidegger, J.M. and Bense, V.F. (2014) Impacts of glacially recharged groundwater flow systems on talik evolution. Journal of Geophysical Research: Earth Surface 119(4), 758-778.

Schlutz, F. and Lehmkuhl, F. (2009) Holocene climatic change and the nomadic Anthropocene in Eastern Tibet: palynological and geomorphological results from the Nianbaoyeze Mountains. Quaternary Science Reviews 28(15-16), 1449-1471.

Schmidt, A., Gibson, J.J., Santos, I.R., Schubert, M., Tattrie, K. and Weiss, H. (2010) The contribution of groundwater discharge to the overall water budget of two typical Boreal lakes in Alberta/Canada estimated from a radon mass balance. Hydrology and Earth System Sciences 14(1), 79-89.

Sebok, E., Duque, C., Kazmierczak, J., Engesgaard, P., Nilsson, B., Karan, S. and Frandsen, M. (2013) High-resolution distributed temperature sensing to detect seasonal groundwater discharge into Lake Væng, Denmark. Water Resources Research 49(9), 5355-5368.

Shaw, R.D. and Prepas, E.E. (1990) Groundwater-lake interactions: I. Accuracy of seepage meter estimates of lake seepage. Journal of Hydrology 119(1–4), 105-120.

Slaymaker, O. (2011) Criteria to distinguish between periglacial, proglacial and paraglacial environments. Quaestiones Geographicae 30(1), 85-94.

Slomp, C.P. and Van Cappellen, P. (2004) Nutrient inputs to the coastal ocean through submarine groundwater discharge: controls and potential impact. Journal of

Hydrology 295(1-4), 64-86.

Smerdon, B., Mendoza, C. and Devito, K. (2007) Simulations of fully coupled lake-groundwater exchange in a subhumid climate with an integrated hydrologic model. Water Resources Research 43(1).

Stets, E.G., Winter, T.C., Rosenberry, D.O. and Striegl, R.G. (2010) Quantification of surface water and groundwater flows to open- and closed-basin lakes in a headwaters watershed using a descriptive oxygen stable isotope model. Water Resources Research 46(3).

Tockner, K., Malard, F., Uehlinger, U. and Ward, J. (2002) Nutrients and organic matter in a glacial river-floodplain system (Val Roseg, Switzerland). Limnology and Oceanography 47(1), 266-277.

Valiela, I., Teal, J.M., Volkmann, S., Shafer, D. and Carpenter, E.J. (1978) Nutrient and Particulate Fluxes in a Salt-Marsh Ecosystem - Tidal Exchanges and Inputs by Precipitation and Groundwater. Limnology and Oceanography 23(4), 798-812.

Wang, C., Dong, Z., Qin, X., Zhang, J., Du, W. and Wu, J. (2016a) Glacier meltwater runoff process analysis using δD and $\delta^{18}O$ isotope and chemistry at the remote Laohugou glacier basin in western Qilian Mountains, China. Journal of Geographical Sciences 26(6), 722-734.

Wang, J., Zhu, L., Wang, Y., Ju, J., Xie, M. and Daut, G. (2010) Comparisons between the chemical compositions of lake water, inflowing river water, and lake sediment in Nam Co, central Tibetan Plateau, China and their controlling mechanisms. Journal of Great Lakes Research 36(4), 587-595.

Wang, R., Liu, Z., Jiang, L., Yao, Z., Wang, J. and Ju, J. (2016b) Comparison of surface water chemistry and weathering effects of two lake basins in the Changtang Nature Reserve, China. Journal of Environmental Sciences 41, 183-194.

Wang, S. (1997) Frozen ground and environment in the Zoige Plateau and its surrounding mountains (In Chinese with English abstract). Journal of Glaciology and Geocryology 19(1), 39-46.

Warner, N.R., Christie, C.A., Jackson, R.B. and Vengosh, A. (2013) Impacts of shale gas wastewater disposal on water quality in western Pennsylvania. Environmental Science & Technology 47(20), 11849-11857.

Weynell, M., Wiechert, U. and Zhang, C. (2016) Chemical and isotopic (O, H, C) composition of surface waters in the catchment of Lake Donggi Cona (NW China) and implications for paleoenvironmental reconstructions. Chemical Geology 435, 92-107.

White, D., Lapworth, D.J., Stuart, M.E. and Williams, P.J. (2016) Hydrochemical profiles in urban groundwater systems: New insights into contaminant sources and pathways in the subsurface from legacy and emerging contaminants. Science of the Total Environment 562, 962-973.

Wilson, J. and Rocha, C. (2016) A combined remote sensing and multi-tracer approach for localising and assessing groundwater-lake interactions. International Journal of Applied Earth Observation and Geoinformation 44, 195-204.

Winter, T.C. (1999) Relation of streams, lakes, and wetlands to groundwater flow systems. Hydrogeology Journal 7(1), 28-45.

Wischnewski, J., Herzschuh, U., Rühland, K.M., Bräuning, A., Mischke, S., Smol, J.P. and Wang, L. (2014) Recent ecological responses to climate variability and human impacts in the Nianbaoyeze Mountains (eastern Tibetan Plateau) inferred from pollen, diatom and tree-ring data. Journal of Paleolimnology 51(2), 287-302.

Xin, W., Yongjian, D., Shiyin, L., Lianghong, J., Kunpeng, W., Zongli, J. and Wanqin, G. (2013) Changes of glacial lakes and implications in Tian Shan, central Asia, based on remote sensing data from 1990 to 2010. Environmental Research Letters 8(4), 044052.

Yang, K., Wu, H., Qin, J., Lin, C., Tang, W. and Chen, Y. (2014) Recent climate changes over the Tibetan Plateau and their impacts on energy and water cycle: A review. Global and Planetary Change 112, 79-91.

Yao, T., Masson-Delmotte, V., Gao, J., Yu, W., Yang, X., Risi, C., Sturm, C., Werner, M., Zhao, H., He, Y., Ren, W., Tian, L., Shi, C. and Hou, S. (2013) A review of climatic controls on $\delta^{18}O$ in precipitation over the Tibetan Plateau: Observations and simulations. Reviews of Geophysics 51(4), 525-548.

Yao, T., Thompson, L., Yang, W., Yu, W., Gao, Y., Guo, X., Yang, X., Duan, K., Zhao, H., Xu, B., Pu, J., Lu, A., Xiang, Y., Kattel, D.B. and Joswiak, D. (2012) Different glacier status with atmospheric circulations in Tibetan Plateau and surroundings. Nature Clim. Change 2(9), 663-667.

Yao, Z., Wang, R., Liu, Z., Wu, S. and Jiang, L. (2015) Spatial-temporal patterns of major ion chemistry and its controlling factors in the Manasarovar Basin, Tibet. Journal of Geographical Sciences 25(6), 687-700.

Yuan, H., Liu, E., Shen, J., Zhou, H., Geng, Q. and An, S. (2014) Characteristics and origins of heavy metals in sediments from Ximen Co Lake during summer monsoon season, a deep lake on the eastern Tibetan Plateau. Journal of Geochemical Exploration 136, 76-83.

Zhang, B., Wu, Y., Zhu, L., Wang, J., Li, J. and Chen, D. (2011) Estimation and trend detection of water storage at Nam Co Lake, central Tibetan Plateau. Journal of Hydrology 405(1-2), 161-170.

Zhang, C. and Mischke, S. (2009) A Lateglacial and Holocene lake record from the Nianbaoyeze Mountains and inferences of lake, glacier and climate evolution on the eastern Tibetan Plateau. Quaternary Science Reviews 28(19), 1970-1983.

Zhang, G., Yao, T., Piao, S., Bolch, T., Xie, H., Chen, D., Gao, Y., O'Reilly, C.M., Shum, C.

and Yang, K. (2017a) Extensive and drastically different alpine lake changes on Asia's high plateaus during the past four decades. Geophysical Research Letters 44(1), 252-260.

Zhang, G., Yao, T., Shum, C., Yi, S., Yang, K., Xie, H., Feng, W., Bolch, T., Wang, L. and Behrangi, A. (2017b) Lake volume and groundwater storage variations in Tibetan Plateau's endorheic basin. Geophysical Research Letters 44(11), 5550-5560.

Zhang, G., Yao, T., Xie, H., Kang, S. and Lei, Y. (2013) Increased mass over the Tibetan Plateau: from lakes or glaciers? Geophysical Research Letters 40(10), 2125-2130.

Zhang, Y., Liu, C., Tang, Y. and Yang, Y. (2007) Trends in pan evaporation and reference and actual evapotranspiration across the Tibetan Plateau. Journal of Geophysical Research: Atmospheres (1984–2012) 112(D12).

Zhou, S., Kang, S., Chen, F. and Joswiak, D.R. (2013) Water balance observations reveal significant subsurface water seepage from Lake Nam Co, south-central Tibetan Plateau. Journal of Hydrology 491, 89-99.

Zlotnik, V.A., Olaguera, F. and Ong, J.B. (2009) An approach to assessment of flow regimes of groundwater-dominated lakes in arid environments. Journal of Hydrology 371(1), 22-30.

Zlotnik, V.A., Robinson, N.I. and Simmons, C.T. (2010) Salinity dynamics of discharge lakes in dune environments: Conceptual model. Water Resources Research 46(11).

Zongxing, L., Qi, F., Wei, L., Tingting, W., Xiaoyan, G., Zongjie, L., Yan, G., Yanhui, P., Rui, G. and Bing, J. (2015) The stable isotope evolution in Shiyi glacier system during the ablation period in the north of Tibetan Plateau, China. Quaternary International 380, 262-271.

Figure captions

Figure 1 The geological and topographic map of the Yellow River Source Region, Nianbaoyeze glacial mountains (**a**), and the sampling settings of the Ximen Co Lake (**b**), with the bathymetry map of the lake (**d**). (**c**) Photograph of the Ximen Co Lake and the surrounding geomorphic settings looking northeast direction on 22 Aug 2015, showing the late-laying snowpack in the U-shaped valleys of the north part of Nianbaoyeze MT.

Figure 2 The climatological parameters (wind speed, air temperature, and precipitation) in the Aug, 2015 recorded from Jiuzhi weather station.

Figure 3 The temporal distributions of ^{222}Rn (**a**), water temperature (**b**), water level fluctuation recorded by the divers (**c**), and hourly wind speed and air temperature recorded in Jiuzhi weather station (**d**).

Figure 4 The cross plots of Cl^- versus Na^+ (**a**), SO_4^{2-} versus Cl^- (**b**), Ca^{2+} versus Cl^- (**c**); The relations of ^{2}H versus ^{18}O (**d**), Cl^- versus ^{2}H (**e**), and Cl^- versus ^{18}O (**f**).

Figure 5 Cross plots of ^{222}Rn versus DIN (**a**) and DIP (**b**).

Figure 6 The conceptual model of ^{222}Rn transient model (**a**), and three endmember model (**b**).

Figure 7 The results of the final LGD derived from ^{222}Rn transient model.

Figure 8 The hydrologic partition of the proglacial lake of Ximen CO (**a**), and the budgets of DIN (**b**) and DIP (**c**).

Figure 1

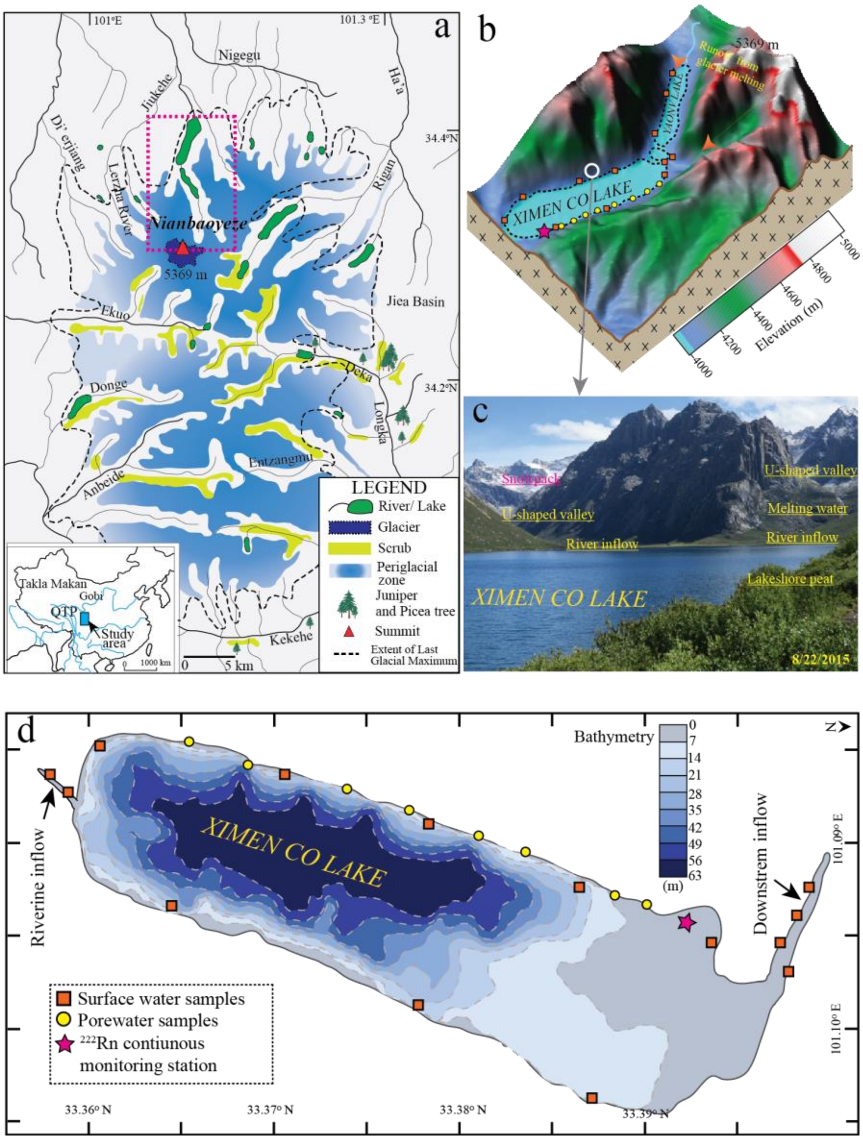
a
101°E
101.3 °E
Nigegu
Jiukehe
Di' erjiang
Ha'a
34.4°N
Rigan
Lerzha River
Nianbaoyeze
5369 m
Ekuo
Jiea Basin
Deka
34.2°N
Donge
Longka
Entzangmu
Anbeide
Kekehe
0
5 km
Takla Makan
Gobi
QTP
Study area
1000 km
LEGEND
River/ Lake
Glacier
Scrub
Periglacial zone
Juniper and Picea tree
Summit
Extent of Last Glacial Maximum
b
5369 m
Runoff from glacier melting
XIMEN CO LAKE
Elevation (m)
4000
4200
4400
4600
4800
5000
c
Snowpack
U-shaped valley
U-shaped valley
Melting water
River inflow
River inflow
Lakeshore peat
XIMEN CO LAKE
8/22/2015
d
Bathymetry
0
7
14
21
28
35
42
49
56
63
(m)
N
XIMEN CO LAKE
Riverine inflow
Downstrem inflow
101.09° E
101.10° E
Surface water samples
Porewater samples
^{222}Rn contiunous monitoring station
33.36° N
33.37° N
33.38° N
33.39° N

Figure 2

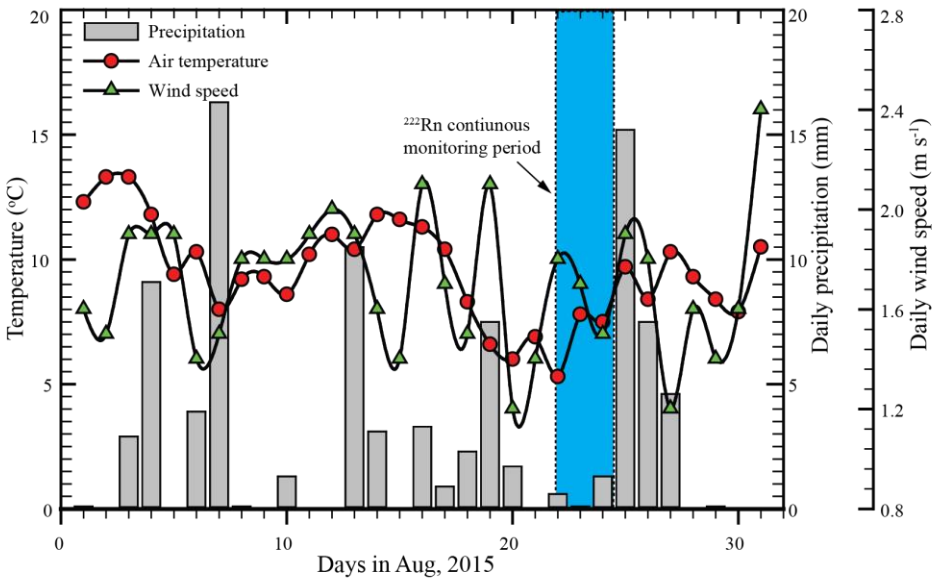

Precipitation
Air temperature
Wind speed
^{222}Rn contiunous
monitoring period
Temperature (°C)
Daily precipitation (mm)
Daily wind speed (m s^{-1})
Days in Aug, 2015
0
5
10
15
20
25
30
0.8
1.2
1.6
2.0
2.4
2.8

Figure 3

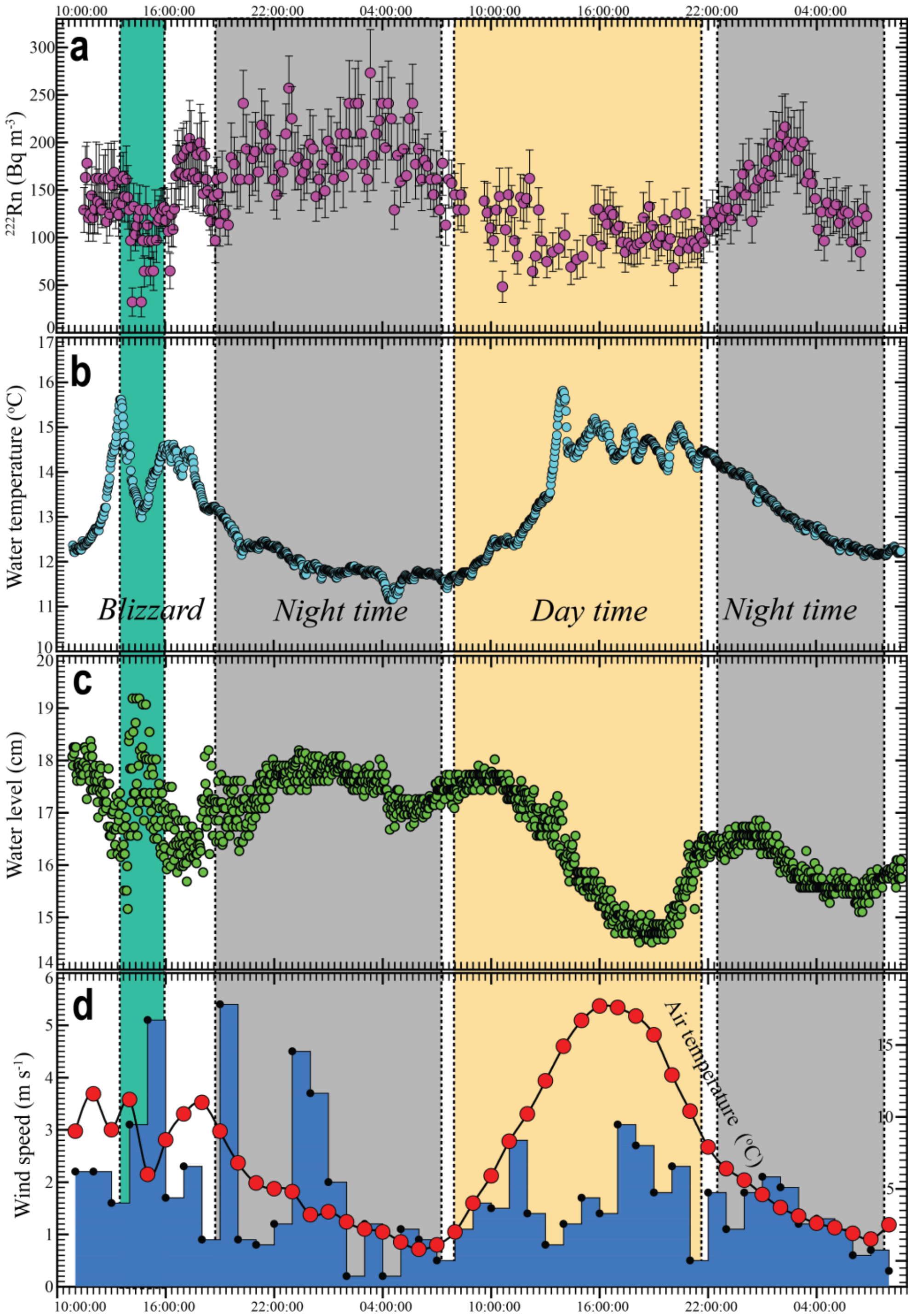

a
^{222}Rn (Bq m^{-3})
b
Water temperature (°C)
Blizzard
Night time
Day time
Night time
c
Water level (cm)
d
Wind speed (m s^{-1})
Air temperature (°C)
10:00:00
16:00:00
22:00:00
04:00:00
10:00:00
16:00:00
22:00:00
04:00:00

Figure 4

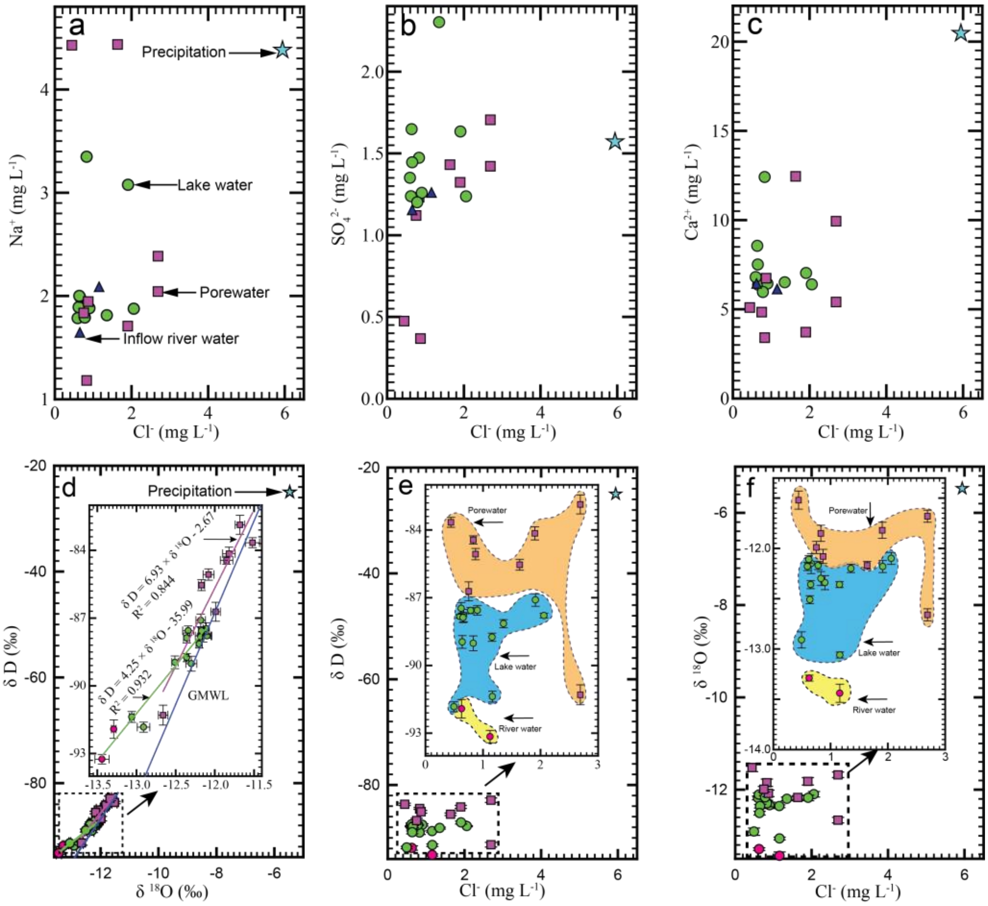

a
Precipitation
Lake water
Porewater
Inflow river water
Na+ (mg L-1)
Cl- (mg L-1)
b
SO4 2- (mg L-1)
Cl- (mg L-1)
c
Ca2+ (mg L-1)
Cl- (mg L-1)
d
Precipitation
δ D = 6.93 × δ 18O - 2.67
R2 = 0.844
δ D = 4.25 × δ 18O - 35.99
R2 = 0.932
GMWL
δ D (‰)
δ 18O (‰)
e
Porewater
Lake water
River water
δ D (‰)
Cl- (mg L-1)
f
Porewater
Lake water
River water
δ 18O (‰)
Cl- (mg L-1)

Figure 5

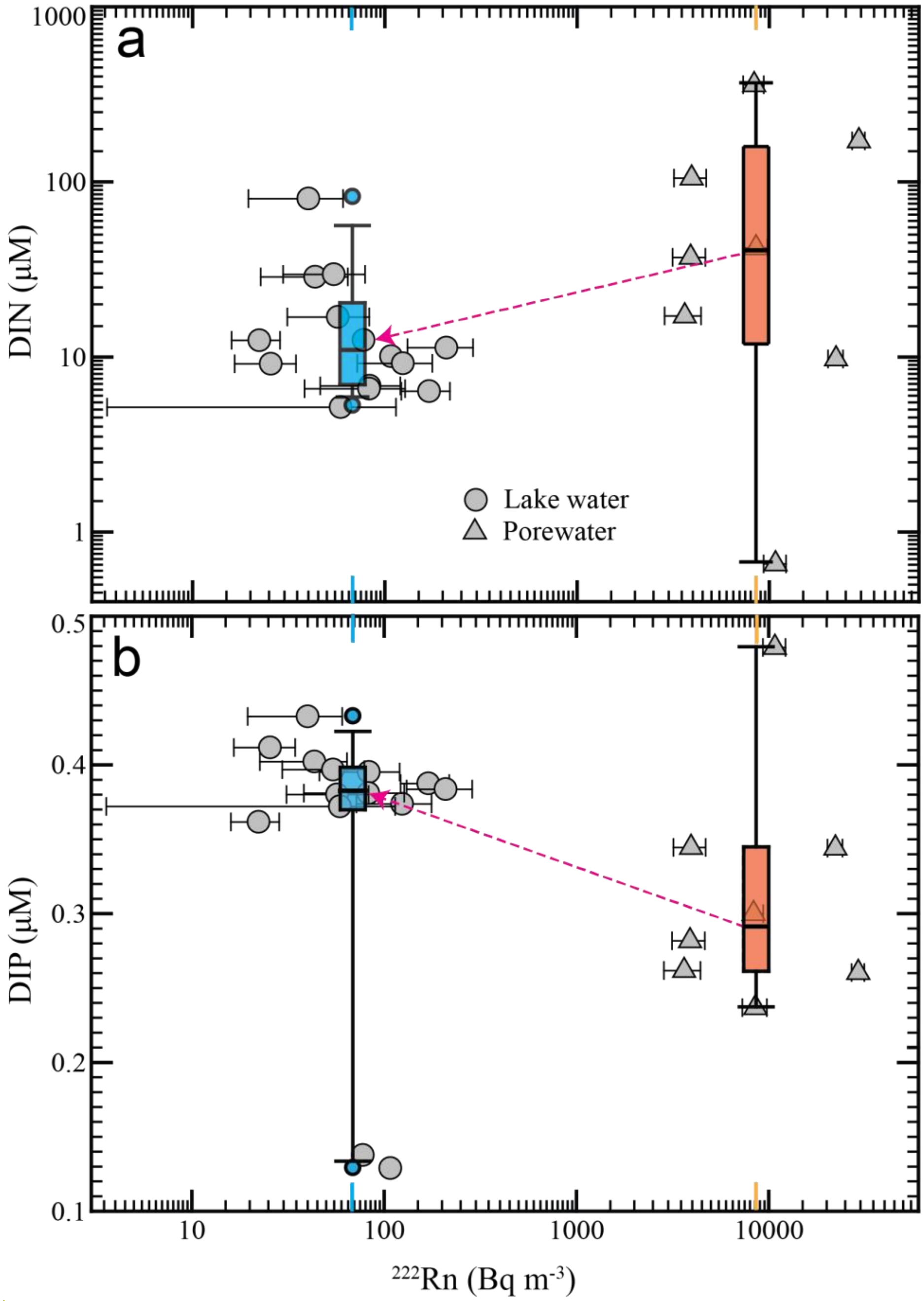

Formatted: Font: (Default) Times New Roman, (Asian) 宋体, 11 pt

Formatted: Indent: Left: 0 cm, Hanging:

Figure 6

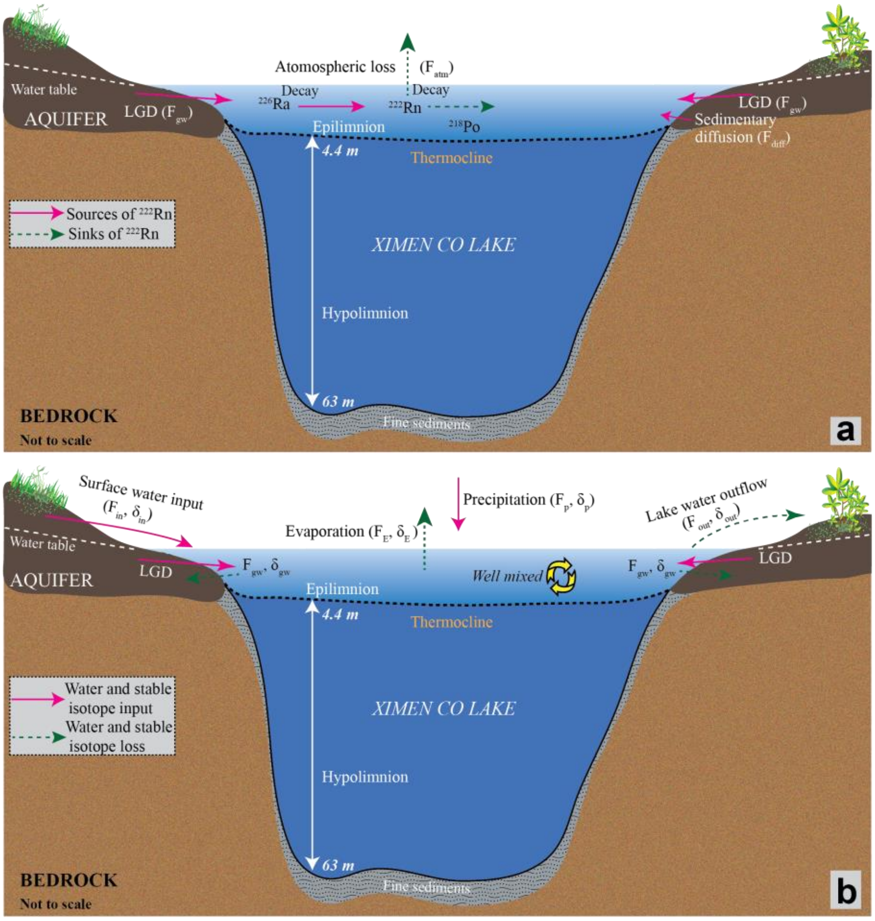

Deleted:

Figure 7

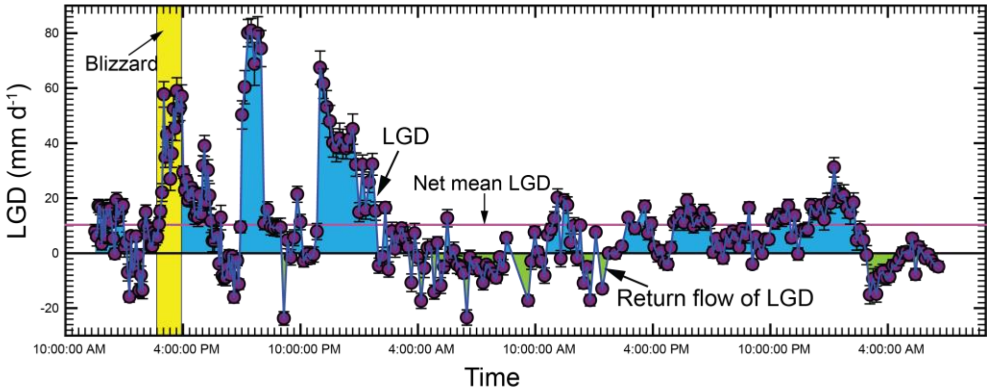
Blizzard
LGD
Net mean LGD
Return flow of LGD
LGD (mm d-1)
80
60
40
20
0
-20
10:00:00 AM
4:00:00 PM
10:00:00 PM
4:00:00 AM
10:00:00 AM
4:00:00 PM
10:00:00 PM
4:00:00 AM
Time

Figure 8

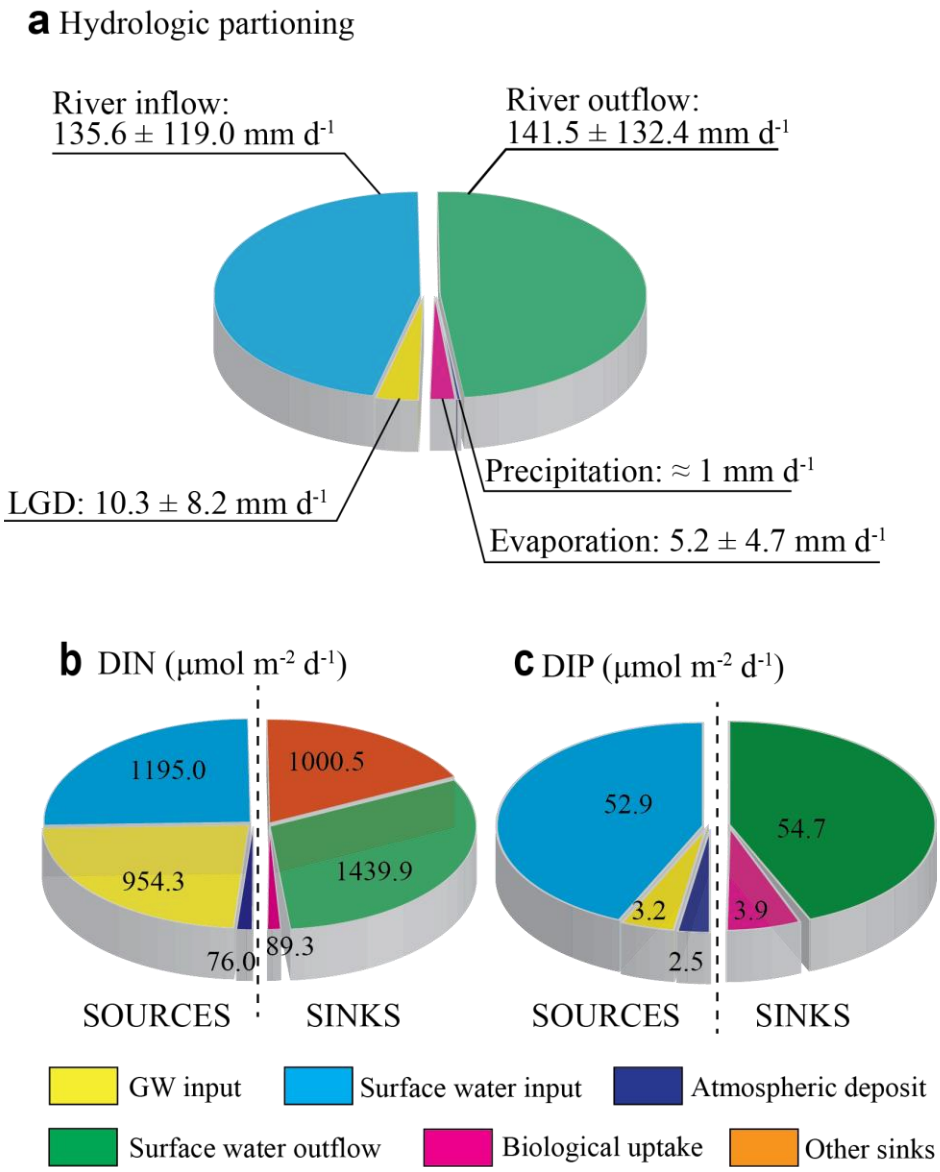
a Hydrologic partioning
River inflow:
135.6 ± 119.0 mm d-1
River outflow:
141.5 ± 132.4 mm d-1
Precipitation: ≈ 1 mm d-1
LGD: 10.3 ± 8.2 mm d-1
Evaporation: 5.2 ± 4.7 mm d-1
b DIN (μmol m-2 d-1)
1195.0
1000.5
954.3
1439.9
76.0
89.3
SOURCES
SINKS
c DIP (μmol m-2 d-1)
52.9
54.7
3.2
3.9
2.5
SOURCES
SINKS
GW input
Surface water input
Atmospheric deposit
Surface water outflow
Biological uptake
Other sinks